International Astronomy and Astrophysics Research Journal

Volume 5, Issue 1, Page 150-183, 2023; Article no.IAARJ.104555

Photometric Analysis for Searching Variable Stars in the Field of the Northern Open Cluster NGC 1960

Gireesh Chandra Joshi [a*]

[a] *Department of Physics, Government Degree College, Kanvaghati, Kotdwar, Uttarakhand, India.*

Author's contribution

The sole author designed, analysed, interpreted and prepared the manuscript.

Article Information

Open Peer Review History:
This journal follows the Advanced Open Peer Review policy. Identity of the Reviewers, Editor(s) and additional Reviewers, peer review comments, different versions of the manuscript, comments of the editors, etc are available here: https://www.sdiarticle5.com/review-history/104555

Received: 12/06/2023
Accepted: 16/08/2023
Published: 02/09/2023

Original Research Article

ABSTRACT

The aim of the present work is to extract and analyses the light curves of the stars in the field of the cluster, NGC 1960. The photometric calibration is performed by a comprehensive method of secondary standard transformation alongwith differential photometry using two comparison stars per candidate variable star. The resultant light curves for each potential variable star are displayed and their period are analyzed by two different methods. The period and classification of the 18 discovered short periodic type variable stars of NGC 1960 are discussed, which consist of four known variable stars and fourteen new variable stars. Among the eighteen detected variables of NGC 1960, one as $\gamma - Dor$, one as RR Lyre, two as EB, two as Ellipsoidal, two as hybrid ($\delta\ Scuti - \gamma - Dor$), two as LADS, two as rotational and six as irregular or miscellaneous type variable stars. In the case of NGC 1960, the 12 selected comparison stars appear to be likely candidate for long periodic variability, and four stars may be possible candidate for standard stars. The variation in brightness of the other twenty comparison stars is non-pulsating with an irregular pattern. Mean proper motions of the core region of NGC1960 are $\bar{\mu_x} = 0.314 \pm 0.026\ mas/yr$ and $\bar{\mu_y} = -2.333 \pm 0.037\ mas/yr$ in the R.A. and DEC. directions, respectively.Membership analysis of variable stars is performed using their distance, kinematic probability and location in $(U - B)$ vs $(B - V)$ TCD. C-M diagrams were constructed to confirm the evolutionary state of the new variable stars.

Corresponding author: E-mail: gshunyansh@gmail.com;

Keywords: Astronomical reduction – NGC 1960; stellar variability.

1 INTRODUCTION

The stars of Population-I are found in Open Star Clusters (OCLs). The fluctuations in brightness found for some stars among members of stellar population and such stars are known as variable stars. The stellar variability arise either due to intrinsic properties (pulsations, eruptions, stellar swelling and shrinking) or due to extrinsic reasons (eclipsed by stellar rotation by another star or planet etc.). Their census, including pulsators and binaries can provide important clues to stellar evolution and the host star clusters [1]. The several classes of pulsating variables are found extensively in the instability strip region of the Hertzsprung-Russell (HR) diagram. Since pulsating variables above the main sequence (MS) have an associated instability strip [2], therefore, a star cluster provides an opportunity to estimate the properties of its stellar variables through its own characteristic parameters.

Since the detection and magnitude estimation of the fainter stars are primarily affected by their nearby brighter stars, knowledge of the flux contamination of the stars in the science frame of any cluster is useful for probing the nature of instrumental pseudo-variability. For such a study, a cluster region consisting of bright stars is required, and NGC 1960 has been found to be a likely candidate for such a study.

In this background, the time series observations of NGC 1960 have been analyzed to search the variable stars within them. The previous parametric studies of this cluster is given in Section 2. The observational details are given in Section 3. The methodology of data reduction is discussed in Section 4. The identification procedure for variable stars in NGC 1960 is given in Section 5. Fast-Fourier analysis of variables discussed in Section 6. Mean-proper motions and kinematics membership probabilities are described in Section 7. A comparative study of variable stars of cluster, NGC 1960 with its parameters are discussed in Section 8. A detail description of the identified stars in the cluster NGC 1960 is given in Section 9. The results, discussion and Conclusion are described in Sections 10 & 11.

2 PREVIOUS STUDIES AND ANTECEDENTS OF STELLAR VARIABILITY FOR NGC 1960

This cluster is located in the Constellation Auriga. The Center coordinates $(\alpha,\ \delta)$ for this cluster have been calculated by Sharma et al.[3] and Cantat & Anders [4] as $(05^h : 36^m : 20.8^s,\ +34^o : 08^{'} : 31^{"})$ and $(05^h : 36^m : 20.2^s,\ +34^o : 08^{'} : 06^{"})$, respectively. Its angular size is computed by Cantat & Anders [4] and Joshi & Tyagi [5] as 10.3 arcmin and 16 arcmin, respectively. Previously, this cluster was studied by various research groups [3, 6, 7, 8, 9, 10, 11, 12, 13, 14].

A complete $UBVRIJHKW_1W_2$ photometric catalogue has been represented by Joshi & Tyagi [5] by complying with the PPMXL catalogue and obtained $UBVRI$ standard photometric magnitude of data collected on date of 30 Nov, 2010 and the data set was further analyzed by JO20 for their absolute or standard photometric analysis. By utilizing catalogs of various data-sets, a comprehensive photometric analysis of this cluster with the long-term variability is shown by them. A total of 76 variable stars from the Filed-of-View (FoV) of NGC 1960 have been identified by JO20, and their analysis confirmed 72 periodic variables, 59 of which are short period $(P < 1\ d)$. They have used absolute phtometry to detect variable stars, to which instrumental errors are surely added due to magnitude transformation. In the case of J20's dataset, there are only three data strings of continuous time series observation with a gape of more than 1 year and length of each data string is less than 3.5 hours (i.e. $\simeq$ 0.146 d). Time gape of more than 1 year leads additional aliases. Mostly, other observational nights have only 1-3 frames with irregular exposure time as well as time interval, which do not seem suitable for the detection of short periodic variable stars. Thus, it is impossible to determine a short periodic variable star.

In the case of this cluster, flux of fainter stars would be contaminated due to over-flow flux of nearby brighter stars during its deep CCD photometric observations. Such circumstances surely lead to an over-estimation in the detection of short periodic variable stars. In view of the above antecedent, the author is also motivated

to perform time series observations of this cluster with short exposure times of 05, 06 and 10 seconds.

3 DATA COLLECTION, EXTRACTION AND CHARACTERISTICS OF OBSERVATIONAL DATA OF NGC 1960

To detect the short periodic pulsation of stars in the target cluster, we need time series observation of the whole night as per the availability of the target in the telescopic field of view. The time series observations of the studied cluster NGC 1960 are carried out using the observational facilities of the 1.04-m Sampurnand telescope of ARIES, Manora Peak, Nainital. The CCD camera of 1.04-m Sampunanad telescope of ARIES covers $15\times15\ arcmin^2$ field of view of the target object. To identify short periodic pulsations of stars within the core region of NGC 1960, time series observations were carried out in V-band during 5 observation nights (2012-2015). It contains ten stars of a visual magnitude brighter than 10 [9], one B-type Variable of 9^{th} magnitude [15], 178 down to magnitude 14 [13] and 38 members with infrared excess [16]. Thus, there are several bright stars in telescopic field of view for NGC 1960. The author found that these bright stars became nearly saturated during an exposure time of 5 seconds. As a result, the value of exposure time of 5 seconds in V-band becomes too high for saturation counts of the brighter stars of NGC 1960 and leads to flux contamination for nearby fainter stars of bright stars in the observed science frames using the 1.04-m telescope at ARIES, Nainital. Similarly, an exposure time of 1 second is too low value to collect the stellar information for fainter stars in NGC 1960 below 17 mag in V-band. Environmental influences (seeing, air flow, humidity, passing clouds etc.) and high declination of the target cluster from zenith further reduce the value of stellar flux and alter the rate of stellar detection. Therefore, different number of faint stars are detected in different science frames of NGC 1960.

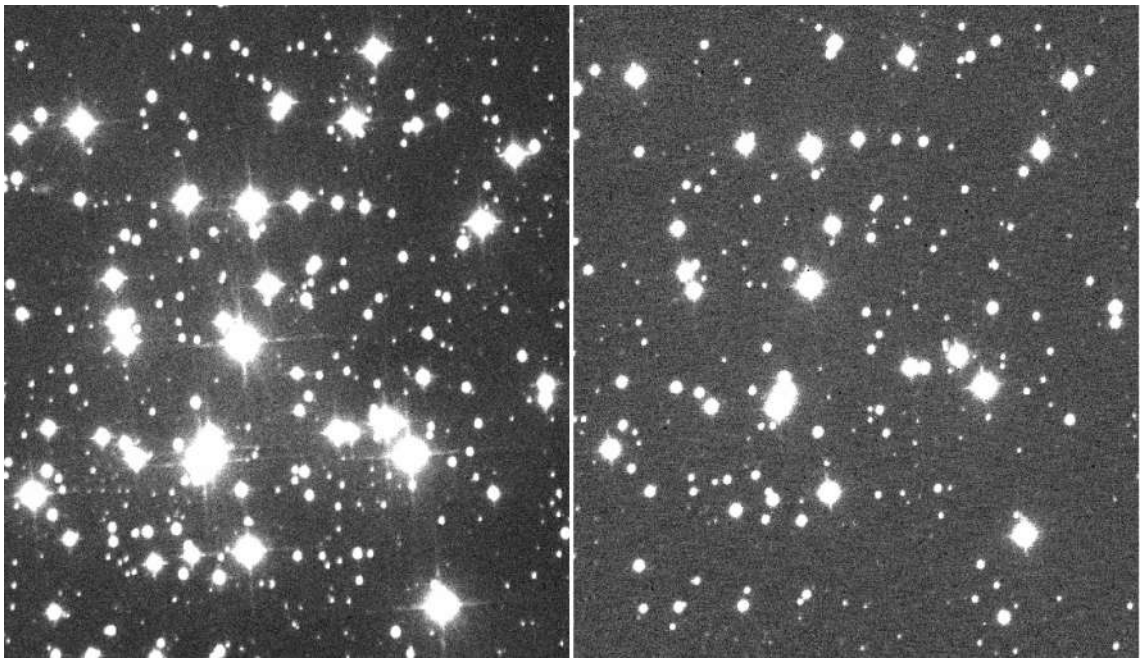

Fig. 1. In the left and right panels of this figure, the science frames of 60 seconds and 10 seconds are shown for core-region of NGC 1960, which are observed on date 24-01-2012 and 11-12-2013 respectively

To overcome the detection problem of faint stars, the author performed a deep CCD photometric observation of the core region of NGC 1960 with exposure times of 10, 20 and 60 seconds. We need continuous observations of 4-6 hours or more, therefore, the science frames of NGC 1960 have been captured in the alternating order of low (5 or 6 seconds) and high (10 or 20 or 60 seconds) exposure times during the observation session at night. Thus, exposure time plays a major role in collecting the stellar information. The visual picture of science frames for exposure times of 10 and 60 seconds for NGC 1960 are shown in the right and left panels of Fig. 1. In addition, the visual picture of science frame for exposure time of 200 seconds is shown in Fig. 2. In these figures, flux contamination of nearby bright stars is found more often in the science frame with exposure times of 60 seconds than that of 10 seconds. The detail of exposure times and a brief description of present data is given in Table 1. After inspecting the light curves of the studied variable stars and their comparison stars in Figs. 4-9, the quality of these curves dated January 24, 2012 and December 20, 2013 is too low to identify the nature of stellar variability. An exposure time of 60 seconds has been kept during the above observations. Thus, the author concludes that observations with exposure times of 05-20 seconds are suitable to analysis the nature of stellar variability within FoV of NGC 1960. In observational sets of 43 nights, JO20 has 1, 1 and 19 observational nights with exposure times of 40, 200 and 60 seconds, respectively. It is noted that the data strings for dated 02/11/2011, 03/11/2011 and 24/12/2012 include observation with an exposure time of 60 seconds. In this background, the classification of variable stars within NGC 1960 by JO20 seems very suspicious.

4 METHODOLOGY OF DATA REDUCTION

Bias correction and flat-fielding of observed science frames of NGC 1960 have been performed using bias and flat frames that were observed in the same observational night of the object. The author also utilized bias and flat frames of nearby night for the science frames of NGC 1960 due to the lack of these frames in the observed data. For this purpose, the 'ZEROCOMBINE' and 'FLATCOMBINE' tasks of 'IRAF' package are used. The 'COSMICRAYS' task of the 'IRAF' software is used to remove cosmic rays from the science frames.

Table 1. The data dated 30/11/2012 and 24/01/2012 for NGC 1960 are common with Joshi & Tyagi (2015) and Joshi et al. (2020), respectively. In the present work, the author collected an additional data-set of 330 frames over 4 nights in the filter V with $t_{exp} = 5 - 60\ sec$ (variable). The observation details of collected data of NGC 1960 for searching variable stars within them.

S.No.	Date	Observation Band (Frames)	Observation Time & Mode	No. of Frames	Exposure Time
1.	30-11-2010	U	–, Slow	002	300 Sec.
		B		002	300 Sec.
		V		002	200 Sec.
		R		002	200 Sec.
		U		002	060 Sec.
2.	24-01-2012	V	3.5 hours, Slow	070	60 Sec.
3.	11-12-2013	V (150 frames)	5.4 hours, Slow	050	05 Sec.
				050	10 Sec.
				050	20 Sec.
4.	20-12-2013	V (080 frames)	7.6 hours, Slow	040	06 Sec.
				040	60 Sec.
5.	12-01-2015	V (200 frames)	7.2 hours, Slow	100	05 Sec.
				100	20 Sec.
6.	08-02-2015	V (140 frames)	5.6 hours, Slow	140	20 Sec.

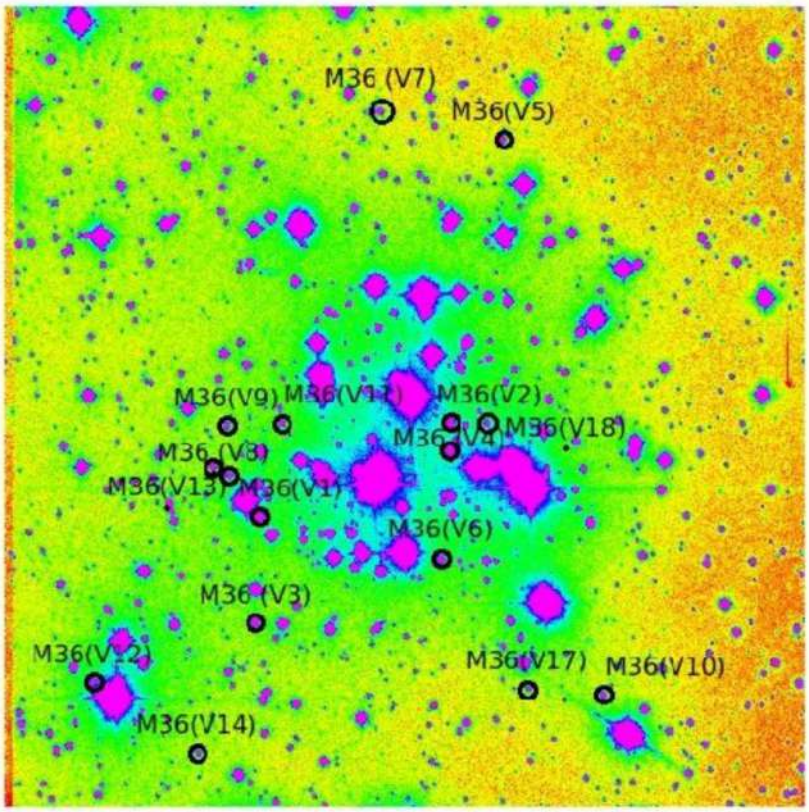

Fig. 2. The science frame for exposure time of 200 seconds is shown for core-region of NGC 1960 (M36) in V-band. It was observed on date 30-11-2010 and taken for process of stellar standardization. The present detected variable stars are depicted by open circle in these Finding charts.

The 'GEOMAP' and 'GEOTRAN' tasks of the IRAF software are used to align the all science frames for analysis. In the astrometry, the pixel coordinates of detected stars are transformed into celestial coordinates ($\alpha_{2000},\ \delta_{2000}$) using a linear astrometric solution derived by matching a set of common stars between present reference catalog and the 2MASS catalog with an rms value of about one arcsec in RA and DEC. A total of 63 common stars have been selected in the observed field of NGC 1960. For this purpose, the visualization of images and access to catalogs have been done by the 'SKYCAT' tool of ESO$*$. The $CCMAP$ and $CCTRAN$ tasks of $IRAF$ were used for these transformation.

4.1 Standardization Details for NGC 1960

To perform consistent photometry from night to night on the aligned images [17], there is need for a master list of stars from the science frames of the cluster that stars have the best seeing and coverage of the observed core region of the cluster, NGC 1960. By using the prescribed telescope in Section 3.1, the photometric observations of the open star cluster NGC 1960 were obtained on the night of November 30, 2010. The bias and twilight flat frames were acquired during the observational night for the normalization of the CCD pixels. The two Landolt's standard fields $SA95$ and $PG0231+051$ [18] were also observed on the same observational night. A total of ten frames of

$*$*www.eso.org/sci/observing*

Table 2. The zeropoint, colour-coefficient and extinction-coefficient for different passbands. The colour-coefficients and extinction coefficients listed here.

Filter	zeropoint(z_i)	colour coefficient(c_i)	extinction coefficient(k_i)
U	8.16 $\pm$ 0.01	-0.05 $\pm$ 0.01	0.55 $\pm$ 0.02
B	5.81 $\pm$ 0.02	-0.01 $\pm$ 0.02	0.29 $\pm$ 0.03
V	5.43 $\pm$ 0.01	-0.08 $\pm$ 0.01	0.15 $\pm$ 0.01
R	5.23 $\pm$ 0.01	-0.09 $\pm$ 0.02	0.09 $\pm$ 0.02
I	5.63 $\pm$ 0.02	0.01 $\pm$ 0.01	0.07 $\pm$ 0.02

the cluster, with 2 frames each in U, B, V, R and I filters, with exposure times of 300, 300, 200, 200 and 60 seconds were obtained. All observations were taken in 2×2 binning mode to improve the signal-to-noise ratio. The basic steps of image processing such as bias subtraction, flat fielding and cosmic-ray removal, were performed through $IRAF$[†]. Photometry analysis was done using $DAOPHOT\ II$ profile fitting software [19]. To quantify the difference between aperture and profile-fitting magnitudes, an aperture growth curve was constructed by $DAOGROW$ program [20]. The instrumental magnitude was translated into standard magnitude using the following transformation equation:

$$m_i = M_i + z_i + c_i \times color + k_i \times X \qquad (4.1)$$

where z_i, c_i, m_i, M_i and k_i are respectively represent the zero-point, colour-coefficient, aperture instrumental magnitude and extinction coefficient of different pass-bands. The $(U-B)$, $(B-V)$, $(V-R)$ and $(R-I)$ colours were used to determine instrumental magnitudes in U, B, V, R and I pass-bands, while X is used for air-mass. The zero-point, colour coefficient and extinction coefficient for $UBVRI$ pass-bands are listed in Table 2.

In Fig. (3a), author has shown the variation of standard deviations with brightness of stars in different pass-bands. It is clear from this figure that the errors increases towards the fainter end. The calibrated residuals in magnitude (difference between standard and calibrated magnitude) of standard stars in the Landolt's field are shown in Fig.(3b). The standard deviation of the calibration are estimated as 0.083, 0.071, 0.047, 0.030 and 0.049 mag in U, B, V, R and I filters, respectively. The present photometry resulted in a total of 1605 stars within $13' \times 13'$ field of the cluster NGC 1960 in which 447, 1088, 1424, 1583 and 1532 stars were found in U, B, V, R and I bands, respectively. The observed field of NGC 1960 is only central region due to the limited field of view of observation facilities. A total of 1194 stars are found to be common between present photometric data with the Sharma et al. (2006) [3]. In the core region of NGC 1960, 409 additional stars have also been detected in present photometry compare that of Sharma et al. (2006) [3]. The stellar magnitudes of the core region of NGC 1960 for $UBVRI$ photometric-system are listed in Table 3.

4.2 Secondary Standardization Method for NGC 1960

In the case of NGC 1960, to translate the stellar magnitudes (as extracted from data on the remaining nights) into absolute magnitudes, differential photometry was performed using the $UBVRI$ catalog of secondary stars. For this purpose, the author used a linear fit between the standard and instrumental magnitudes on each science frame, assuming that most of the stars are non-variables (these non-variable stars also called stable stars). This procedure is defined as the secondary standardization method [SSM [21]]. It is effective to estimate the absolute stellar magnitudes of NGC 1960 through the calibrated magnitudes of its stable stars. The magnitudes of variable stars are rapidly varying compare to other stars, and the identified variable stars were not utilized for such calibration. In this connection, the master list of stable stars of the observed core region of NGC 1960 is prepared.

[†] *Image Reduction and Analysis Facilities (IRAF) is distributed by the National Optical Astronomy Observatories, operated by the Association of Universities for Research in Astronomy Inc., under cooperative agreement with the National Science foundation.*

Table 3. A complete UBVRI catalogue of the stars in the core field of the cluster NGC 1960. Columns 2 and 3 are RA and DEC of stars, respectively in epoch J(2000). From column 4 to 13, author gives photometric magnitudes and corresponding errors in $UBVRI$ passbands.

ID	RA	DEC	U	e_U	B	e_B	V	e_V	R	e_R	I	e_I
1	5:36:03.22	34:03:37.5	10.654	0.005	10.605	0.023	10.449	0.018	10.400	0.003	10.295	0.003
2	5:35:59.29	34:10:27.5	10.322	-	-	-	10.582	-	10.543	-	10.414	-
3	5:36:03.29	34:10:07.9	10.457	-	-	-	10.601	-	10.563	-	10.440	-
4	5:36:34.76	34:03:55.5	10.374	0.004	10.738	0.018	10.636	0.006	10.559	0.004	10.530	0.004
.	.	.	.	.	.	.	.	.	.	.	.	.
9	5:36:08.27	34:14:21.2	12.547	0.005	11.900	0.016	10.900	0.010	-	-	9.762	0.007
10	5:36:22.14	34:07:13.9	11.010	0.003	11.330	0.008	11.165	0.0032	11.082	0.007	11.019	0.004
11	5:36:01.97	34:09:17.7	11.148	0.004	11.382	0.016	11.212	0.007	11.117	0.003	10.999	0.003
12	5:36:15.80	34:14:18.2	11.277	0.004	11.693	0.014	11.235	0.008	10.938	0.008	10.598	0.005
13	5:36:11.54	34:07:06.5	11.145	0.003	11.496	0.009	11.340	0.003	11.274	0.007	11.210	0.005
14	5:35:51.67	34:10:32.6	11.323	0.005	11.539	0.010	11.424	0.007	11.344	0.005	11.243	0.005
15	5:36:07.75	34:09:25.2	11.642	0.003	11.751	0.016	11.524	0.006	11.387	0.004	11.218	0.004
.	.	.	.	.	.	.	.	.	.	.	.	.
.	.	.	.	.	.	.	.	.	.	.	.	.

Table 4. IDs of variable stars for cluster NGC 1960 are listed in first column . V-magnitudes of variable stars of NGC 1960 are given in second column. Values of colour, $(B-V)$, of variable stars of NGC 1960 are listed in third column. Fourth, fifth and sixth columns indicate the difference of magnitudes for potential variable and its comparison stars. Seventh, eighth and ninth columns represent delta differences of prescribed colour values. In case of NGC 1960, V-magnitudes are standard magnitude as reported by Joshi & Tyagi, 2015.

Va. ID.	V-magnitude for Variable V	Colour (B-V) for Variable V	$\Delta_{V_{mag}}$ V & C1	$\Delta_{V_{mag}}$ V & C2	$\Delta_{V_{mag}}$ C1 & C2	$\Delta_{(B-V)}$ V & C1	$\Delta_{(B-V)}$ V & C2	$\Delta_{(B-V)}$ C1 & C2
V_1	14.007 $\pm$ 0.004	0.511 $\pm$ 0.005	-0.032	-0.017	-0.015	-0.164	-0.078	0.086
V_2	14.020 $\pm$ 0.004	0.520 $\pm$ 0.007	0.029	0.044	-0.015	-0.415	-0.152	0.263
V_3	14.127 $\pm$ 0.005	0.991 $\pm$ 0.007	-0.040	-0.011	-0.029	0.418	0.438	0.020
V_4	14.215 $\pm$ 0.008	0.569 $\pm$ 0.008	-0.036	0.019	-0.022	-0.055	-0.145	-0.123
V_5	14.674 $\pm$ 0.006	0.674 $\pm$ 0.007	0.002	0.005	-0.003	-0.013	0.025	0.038
V_6	15.060 $\pm$ 0.004	0.743 $\pm$ 0.006	0.001	0.007	-0.007	-0.088	-0.269	-0.181
V_7	15.155 $\pm$ 0.009	1.522 $\pm$ 0.014	-0.001	0.004	-0.005	0.760	0.509	-0.251
V_8	15.345 $\pm$ 0.005	0.766 $\pm$ 0.005	-0.013	-0.008	-0.005	-0.920	0.072	0.992
V_9	15.497 $\pm$ 0.004	0.938 $\pm$ 0.005	-0.042	0.011	-0.053	-0.164	-1.216	-1.052
V_{10}	15.592 $\pm$ 0.004	0.778 $\pm$ 0.005	0.005	0.022	-0.017	-0.064	-0.027	0.037
V_{11}	15.668 $\pm$ 0.005	0.966 $\pm$ 0.007	-0.034	0.011	-0.045	0.326	-0.103	-0.429
V_{12}	15.711 $\pm$ 0.007	0.946 $\pm$ 0.009	0.089	0.091	0.012	0.135	-0.002	-0.123
V_{13}	15.769 $\pm$ 0.004	0.820 $\pm$ 0.006	-0.001	0.031	0.009	-0.364	-0.032	0.373
V_{14}	15.969 $\pm$ 0.004	0.944 $\pm$ 0.007	-0.017	0.001	-0.018	-0.669	-0.061	0.608
V_{15}	16.197 $\pm$ 0.005	0.809 $\pm$ 0.008	-0.002	0.016	-0.018	-0.387	-0.217	0.170
V_{16}	16.279 $\pm$ 0.006	0.984 $\pm$ 0.008	0.022	0.041	-0.019	-0.001	-0.709	-0.708
V_{17}	16.369 $\pm$ 0.007	1.070 $\pm$ 0.011	-0.007	0.022	-0.029	0.285	-0.840	-1.125
V_{18}	16.673 $\pm$ 0.007	1.112 $\pm$ 0.009	-0.007	0.006	-0.013	0.242	0.224	-0.018

5 IDENTIFICATION OF VARIABLE STARS

The shapes of light curves of a variable star provide valuable information for investigating the nature of stellar variability and underlying physical processes that generate brightness changes. Consequently, the potential variable candidates identify by inspecting of their light curves [22]. If, we find the deviation of absolute magnitudes of star more than 3σ limit of mean value of its light curve, then, it would be considered a possible candidate for variable stars. The amplitude or period of the pulsations can be related to the luminosity of the pulsating stars and the shape of their light curves

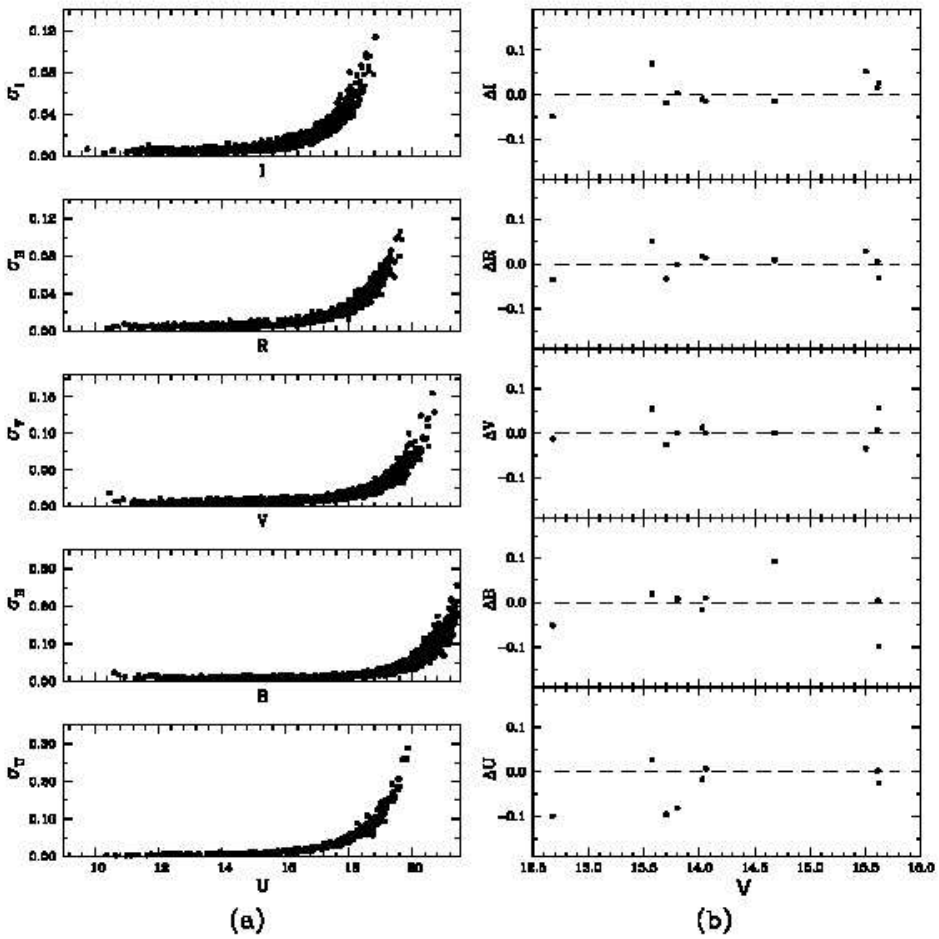

Fig. 3. In left panels, the author presents standard deviation (errors) of stars as a function of brightness. The right panels show difference between estimated magnitudes with that of the Landolt's magnitude for the standard stars in $UBVRI$ passbands. The black dashed line represents zero shift.

can be an indicator of the pulsation mode [23]. As a result, pulsating variables are distinguished by duration of their pulsation and the shapes of their light curves [24]. For this purpose, the applied procedure for searching variable stars is discussed as below,

5.1 Limitation of Differential Photometry in Present Study

It is also noted that effect of contamination depends on exposure times as well as stellar distances from the bright stars. Since, the observed field of NGC 1960 is highly contaminated by the presence of bright stars in its core region, therefore, computed magnitude variation for nearby stars of these bright stars in science frame is varied as per physical distance and stellar orientation. Furthermore, exposure time of its science frames is not constant during observation, which further leads to different amount of flux contamination for them. Even for same exposure time, the flux contamination varies with the distance of cluster from Zenith. As a result, difference of instrumental magnitudes of nearby similar comparison stars is not found approximately constant for detected variables of NGC 1960. The locations of newly identified variable stars are marked by open circles in Fig. 2 and location of their comparison stars are depicted in Figs. 12 and 13.

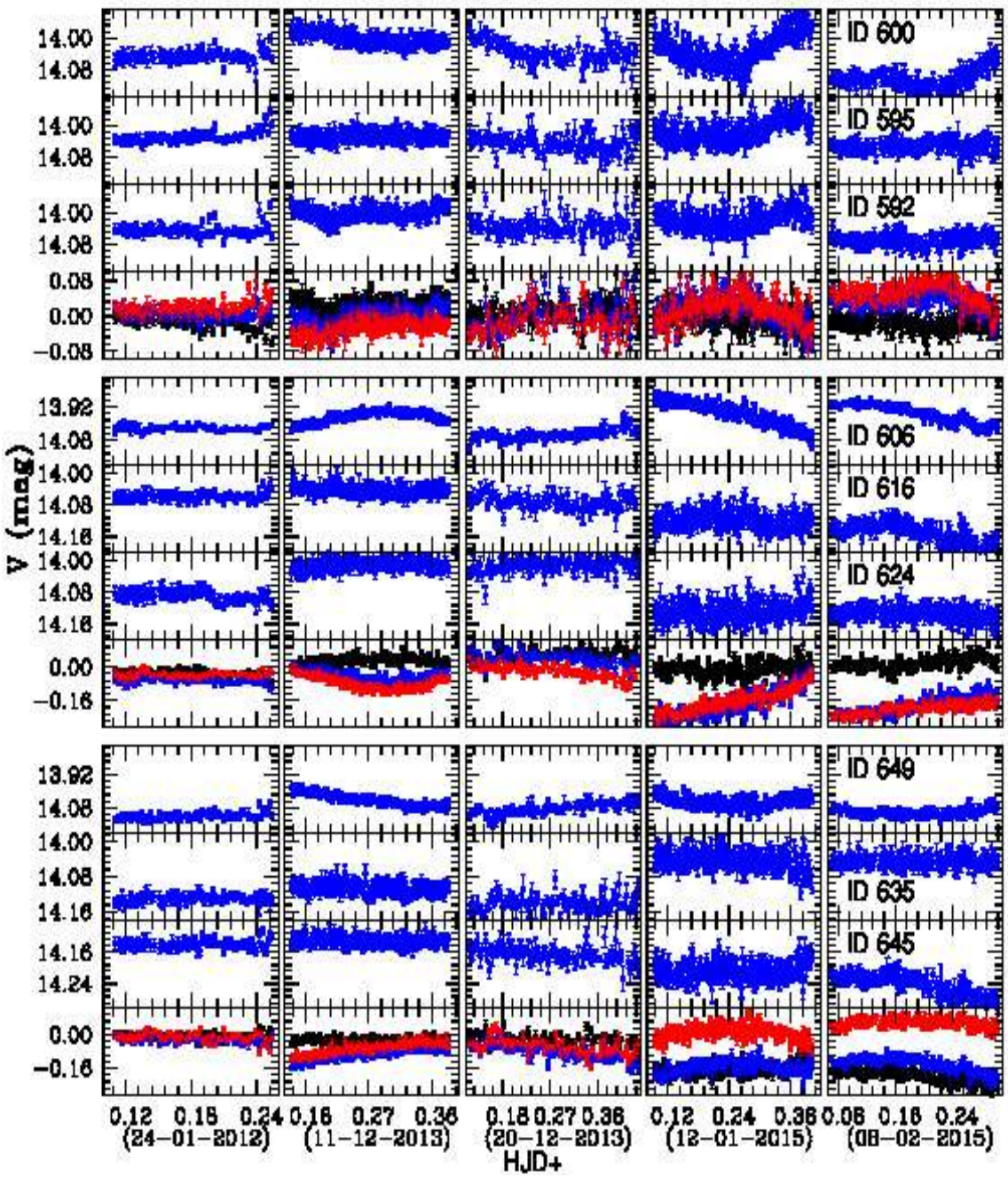

Fig. 4. The panels represent the stellar light curves for star IDs 592, 595, 600, 606, 616, 624, 635, 645 and 649 of cluster NGC 1960. The star IDs 592 and 595 are selected comparison stars for Potential variable (V_1, Star ID 600). The star IDs 616 and 624 are selected comparison stars for Potential variable (V_2, Star ID 606). The star IDs 635 and 645 are selected comparison stars for Potential variable (V_3, Star ID 649).

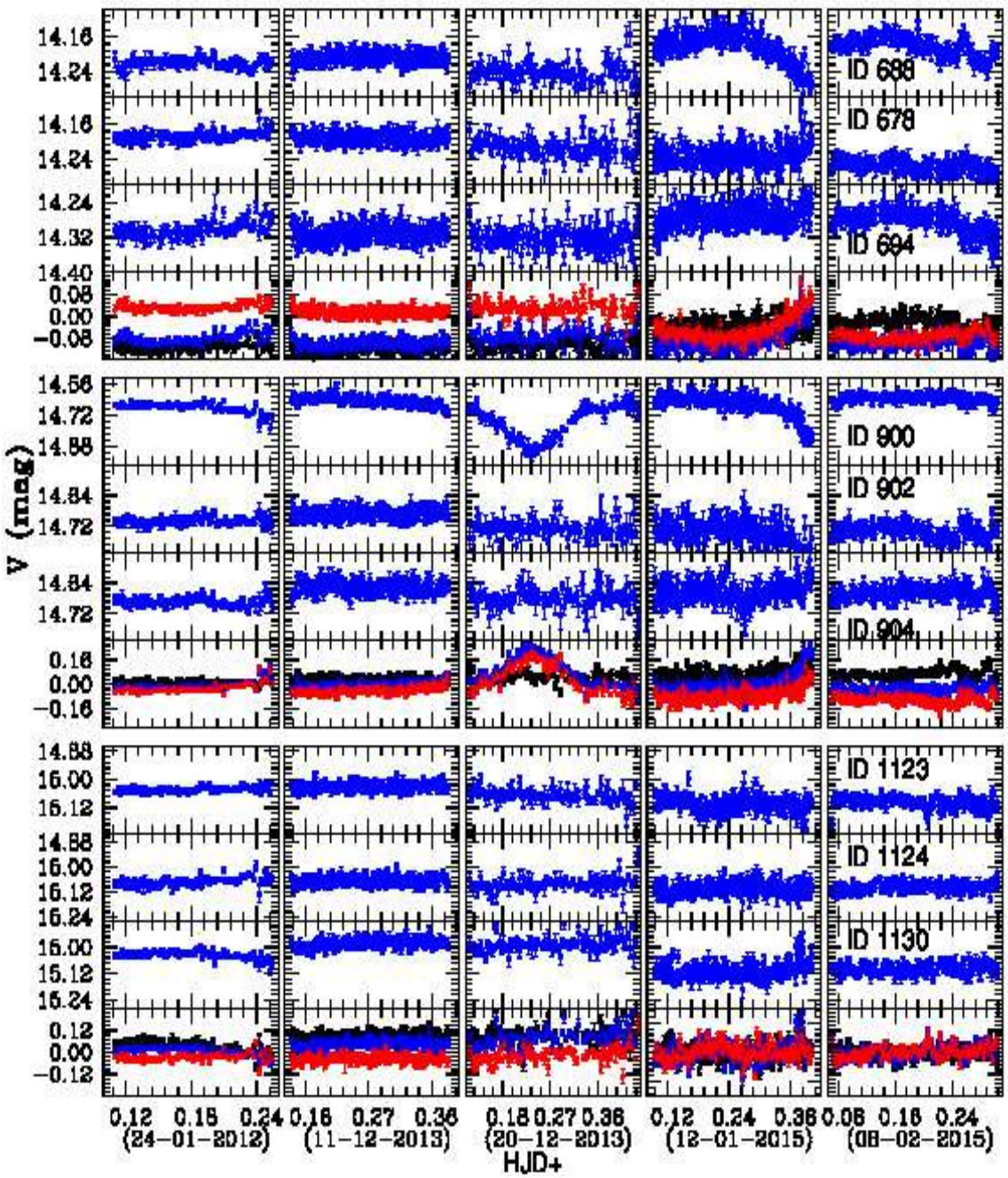

Fig. 5. The panels represent the stellar light curves for star IDs 678, 688, 694, 900, 902, 904, 1123, 1124 and 1130 of cluster NGC 1960. The star IDs 678 and 694 are selected comparison stars for Potential variable (V_4, Star ID 688). The star IDs 902 and 904 are selected comparison stars for Potential variable (V_5, Star ID 900). The star IDs 1124 and 1130 are selected comparison stars for Potential variable (V_6, Star ID 1123).

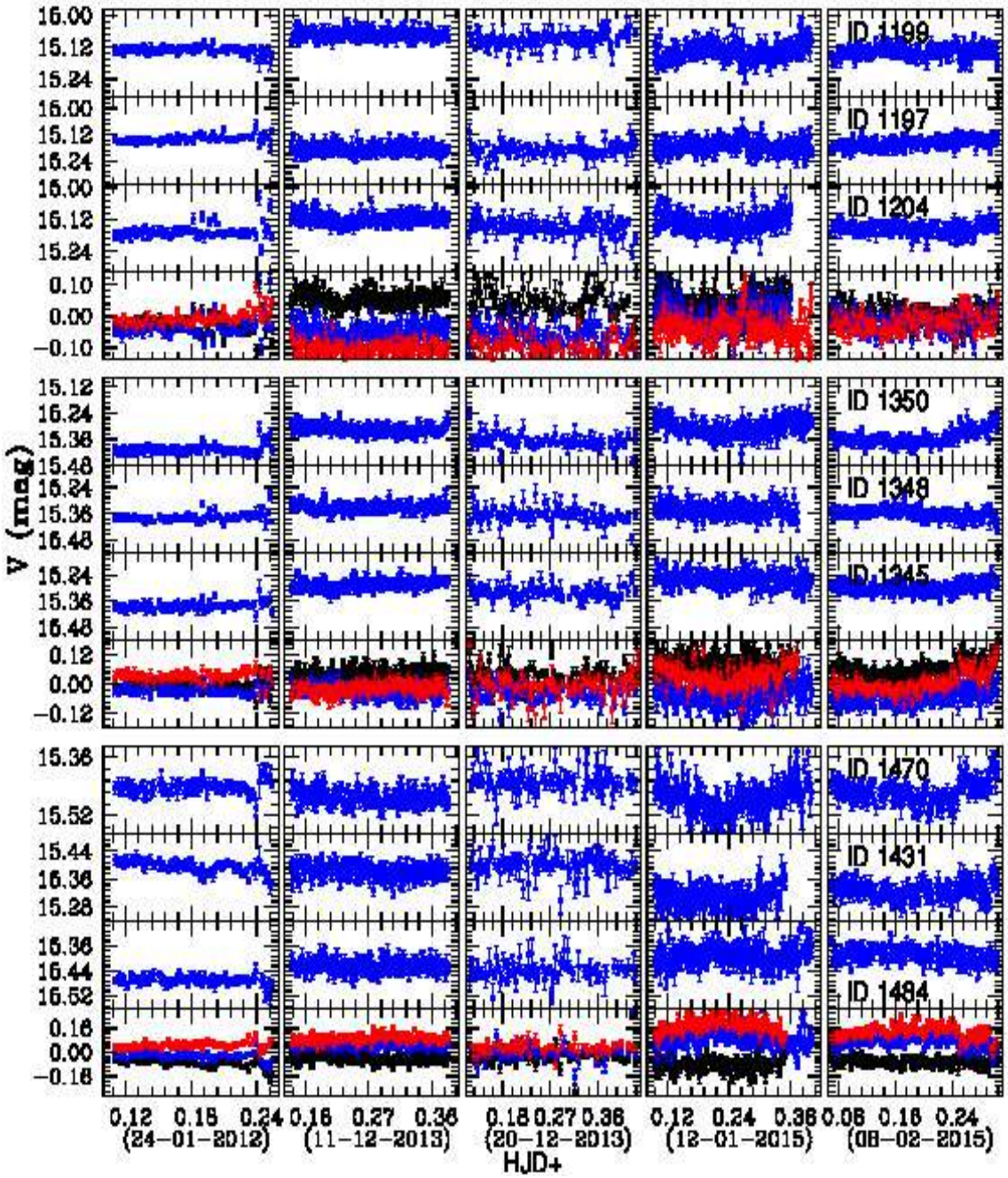

Fig. 6. The panels represent the stellar light curves for star IDs 1197, 1199, 1204, 1345, 1348, 1350, 1431, 1470 and 1484 of cluster NGC 1960. The star IDs 1197 and 1204 are selected comparison stars for Potential variable (V_7, Star ID 1199). The star IDs 1345 and 1348 are selected comparison stars for Potential variable (V_8, Star ID 1350). The star IDs 1431 and 1484 are selected comparison stars for Potential variable (V_9, Star ID 1470)

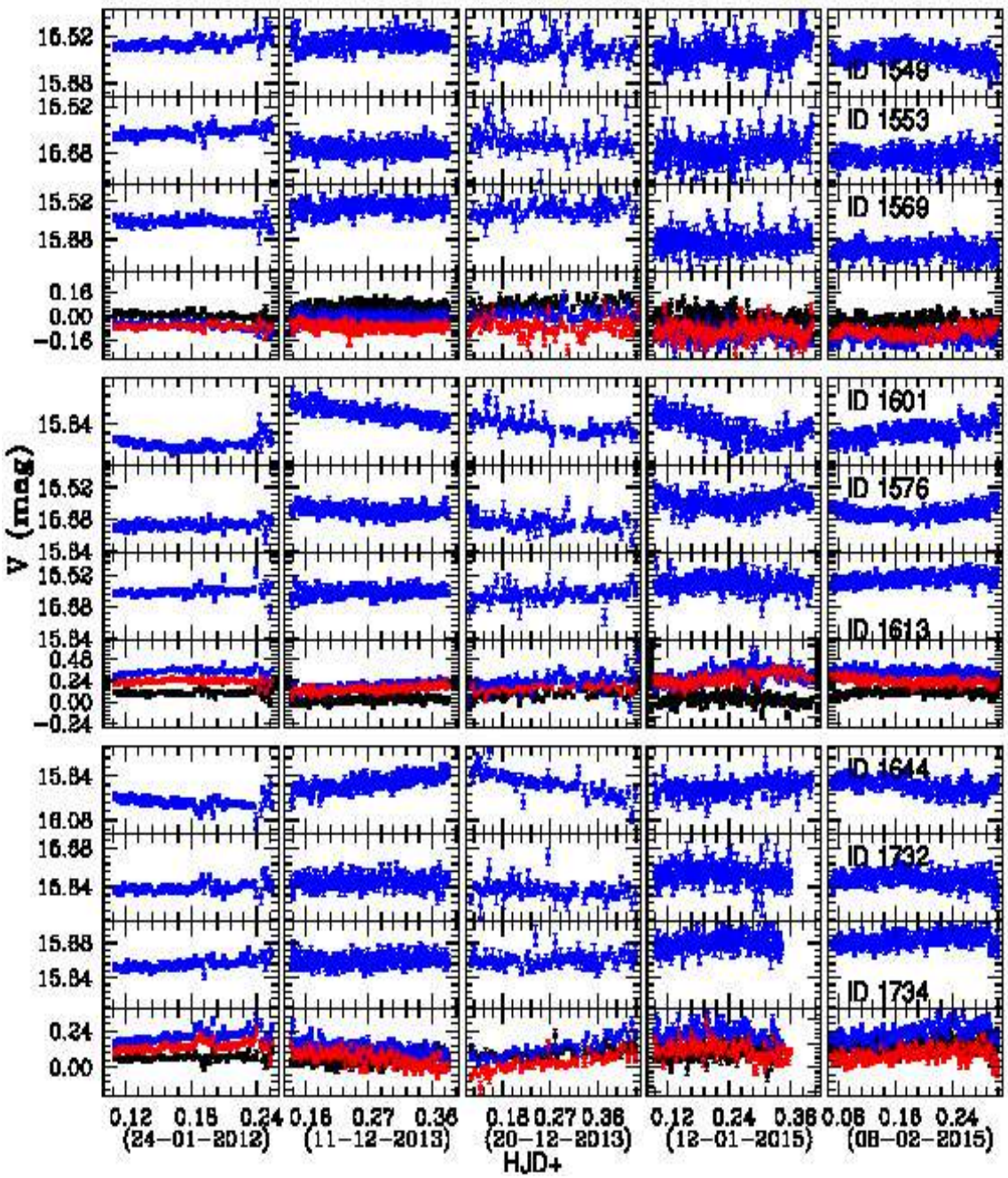

Fig. 7. The panels represent the stellar light curves for star IDs 1549, 1553, 1569, 1576, 1601, 1613, 1644, 1732 and 1734 of cluster NGC 1960. The star IDs 1553 and 1569 are selected comparison stars for Potential variable (V_{10}, Star ID 1549). The star IDs 1576 and 1613 are selected comparison stars for Potential variable (V_{11}, Star ID 1601). The star IDs 1732 and 1734 are selected comparison stars for Potential variable (V_{12}, Star ID 1644).

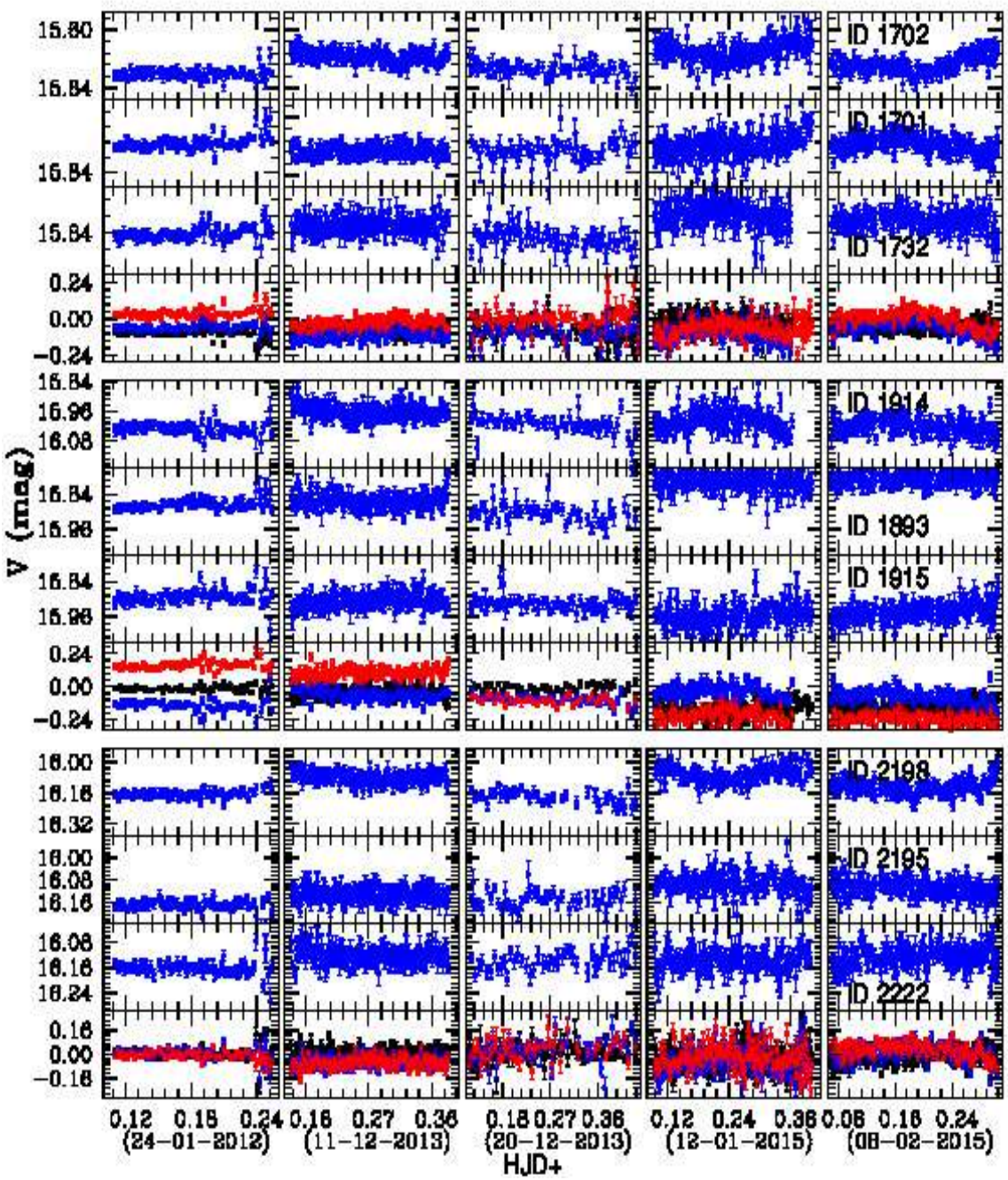

Fig. 8. The panels represent the stellar light curves for star IDs 1701, 1702, 1732, 1893, 1914, 1915, 2195, 2198 and 2222 of cluster NGC 1960. The star IDs 1701 and 1732 are selected comparison stars for Potential variable (V_{13}, Star ID 1702). The star IDs 1893 and 1915 are selected comparison stars for Potential variable (V_{14}, Star ID 1914). The star IDs 2195 and 2222 are selected comparison stars for Potential variable (V_{15}, Star ID 2198).

5.2 Secondary Standardization Methodology and Transformation of Stellar Magnitudes

The transformation of apparent magnitude of stars into absolute magnitudes is performed through Secondary Standardization Methodology (SSM). During absolute phototmetry, comparison stars are not required for any variable star and have a major advantage over the differential photometry. The number of detected stars of any science frame depends on its exposure time. A total of 1800-3000 stars are found in the science frames of NGC 1960. By applying SSM, the absolute stellar magnitudes is computed to the instrumental magnitudes of each science frame for NGC 1960. In these circumferences, the variables stars are detected after visual inspection of light curves as per standard magnitudes via absolute photometry. The possible candidacies of variable stars are determined for stars, having a variation of amplitudes above the 3σ limit of its mean in light curves. After visual inspection of the light curves of detected stars of studied cluster, the author found a total of 18 possible variable candidates in the observed field of NGC 1960, respectively.

5.3 Limitation of SSM during Search of Variable Stars

The approximate constant environment parameter (seeing, humidity etc.) and dark night is prerequisites for standardization. The sky conditions change unexpectedly, the transformation coefficients during the process of SSM of each science frame also vary accordingly . As a result, errors of computed stellar magnitudes in absolute photometry can be found due to aliases of different sky conditions with the estimation errors of transformation coefficients. In this connection, light curves of stars show some variation in brightness. These variations are very close to estimated stellar magnitudes with respect to standard and reference catalogue. Such variation can also generate the pseudo stellar variability.

These transformed stellar magnitudes are used to generate the light curves of stars. Only those stars are selected as variable stars, that have magnitude variation greater than three times of estimation errors of magnitudes in their light curves as constructed after SSM approach.

5.4 Test of Stellar Variability Via SSM and Differential Photometry

In the present work, the author has not found ideal nearby comparison stars for detected variable stars of studied cluster and only differential photometry is not applicable for such case. Since, no available information of influence of the pseudo variability in detected variables, therefore, author also analysis light curves of stable stars of similar order of magnitudes of variables, for tracing the pattern of pseudo-variability among them.

Since, the transformation of instrumental magnitudes leads additional errors, therefore, the scattering is further increased in data points of their light curves. Such transformation makes a weak information of stellar variability. Thus, it may be possible that a selected stable comparison star has weaker information of stellar variability for any variable star below 3σ limit of its light curves. Consequently, we have been avoided the practice of selection of a single stable star for comparing its light curve that of potential variable. For accuracy, the author has selected two stable comparison stars for each potential variable star within the science frames as observed for cluster. This is done for reducing the effect as found due to magnitude difference of selected comparison stars (possibly stable) and their corresponding variable stars.

The pixel distance, differences of stellar magnitudes and colours of identified variables and their comparison stars are listed in the Table 6 and Table 4.

Difference values of pixel coordinates and colours of selected stable stars are consistent with their unusability for study of variable stars via differential photomety. However, comparative analysis of their light curves becomes a tool to understand the nature of instrumental errors and to trace the impact of pseudo-variability. In this background, the differential photometry has been performed to confirm the nature of variable stars above the 3σ limit of variation of instrumental errors of detected stars within NGC 1960.

5.5 Nature of Stellar Light Curves

The light curves of potential variable stars and their corresponding stable stars are shown in Figs. 4 to 9. To distinguish the instrumental variations from stellar light

curves, the stellar magnitudes are subtracted from each other and resulting curves are defined as comparative light curves. The author has applied the differential photometry over absolute photometry to construct such comparative light curves. This process is defined as differential-absolute photometry and effectively reduces the effects in comparative light curves due to sky conditions of observational night.

The light curves for each variable star and its selected comparison stars (set of three stars) have shown in the different panels of these figures. In this connection, each set of stars have four panels. Top panel shows the light curve of potential variables and middle panels show the light curves of selected comparison stars. The fourth panel of each set have three lines of blue, red and black colour to represent the comparative light curves. The blue and red lines are shown the field subtracted light curves of variable through comparison stars, whereas black line represents the difference of stellar magnitudes of selected comparison stars. A constant spacing of comparative light curves is obtained for stable comparison stars, while the varied spacing of these curves confirms the signature of stellar variability. Since, obtained information of stellar variability changes rapidly with the sky and weather conditions, therefore, we can not find stellar variability of the order of $mmag$ during session of bright moon and observational nights, having fog and high humidity. Consequently, we have selected smoothed light curve to compute the period of identified variable stars after the visual inspection of individual light curve of each observational night. The period values are determined by two different methodology as statistical and ANOVA analysis. The period values are not agreeing with each other in 6 cases (V_2, V_3, V_9, V_{10}, V_{12}, V_{15}) among variable stars within Field of View of NGC 1960. In the case of V_2, V_{10} and V_{12} of NGC 1960, both values are seems to be considerable for periodic analysis. It is impossible to determine the true period for variable star V_3 of NGC 1960 as the nightly data strings are about the same computed values.

5.6 Comparative Analysis of SSM with Essential Conditions of Differential Photometry

The major characteristics of the comparative light curves of the present comparison stars of variable stars of NGC 1960 are obtained as below:

(1)- The shifted and varied magnitude differences are found in the comparative light curves of comparison stars of variable stars V_1, V_2 and V_{12} .

(2)- A constant value of magnitude difference is found in the comparative light curves of comparison stars of variable stars V_6, V_8 and V_{11} during observations of individual night. However, shifting of magnitude difference is altered from night to night.

(3)- A constant value of magnitude differences is found in the comparative light curves of comparison stars of variable stars V_3, V_4, V_9, V_{14} and V_{17} during the observations on January 24, 2012, December 11, 2013 and December 20, 2013. Similarly, a shifted and constant value of magnitude differences was obtained in the light curves of these stars during the observations on January 12, 2015 and February 08, 2015.

(4)- A constant value of magnitude differences is found in the comparative light curves of comparison stars of variable stars V_5, V_9, V_{10}, V_{13}, V_{15}, V_{16} and V_{18} during the observations.

Thus, the detected variable stars of NGC 1960 are listed in four different groups as per the comparative light curves of their comparison stars. After deep investigation of Table 6 and Table 4, we did not find any criteria for the geometric distribution of comparison stars and their colour-difference values for separating variable stars of NGC 1960 into these obtained groups. It indicates that there is no need of comparison stars for any variable star after implication of SSM approach. In a nutshell, the present SSM approach is seems to be reliable for evaluating the nature of stellar variable within studied clusters.

6 FOURIER TRANSFORM OF VARIABLES AND THEIR PULSATIONS

Aliases frequencies occur in the light curves of stars due to the interaction of the pulsation of variable stars and the noise or instrumental errors. Such summation of noise and pulsation signals of variable stars is removed through the comparison star during differentiate photometry and is an effective method for

Table 5. The first column shows the ID of variable stars within the studied cluster, NGC 1960. The second and third columns represent RA and DEC respectively. The values of the period of detected variable stars are estimated through the PERIOD04 and PerSea Software, as listed in the fourth and seventh columns, respectively.

Variable ID	RA ($J2000$)	DEC ($J2000$)	Period (days) PERIOD04	Amplitude (mmag)	Power [PERIOD04]	Period (days) PerSea
V_1	$05:36:25.11$	$34:06:10.2$	0.3057 ± 0.0815	102	66.948	0.4000 ± 0.1055
V_2	$05:36:17.85$	$34:09:14.8$	0.2246 ± 0.0599	165	56.576	0.6250 ± 0.0274
V_3	$05:36:33.33$	$34:06:05.4$	0.3598 ± 0.0001	086	99.261	0.4000 ± 0.2086
V_4	$05:36:20.05$	$34:09:14.6$	0.3115 ± 0.1168	062	35.608	0.2857 ± 0.0706
V_5	$05:35:55.79$	$34:10:07.6$	0.3182 ± 0.0848	248	34.752	0.2857 ± 0.0454 ($2.4949:^{*2}$)
V_6	$05:36:28.54$	$34:09:05.8$	0.1528 ± 0.0194	069	24.174	0.1538 ± 0.0369
V_7	$05:35:53.49$	$34:08:09.6$	0.1747 ± 0.0254	065	23.504	0.1695 ± 0.0154
V_8	$05:36:21.20$	$34:05:25.4$	0.2864 ± 0.0007	073	65.225	0.2857 ± 0.0947
V_9	$05:36:17.96$	$34:05:38.7$	0.2667 ± 0.0006	095	48.289	$0.4629\pm0.0.0399$
V_{10}	$05:36:39.17$	$34:11:42.8$	0.1886 ± 0.0003	074	31.753	0.2404 ± 0.0226
V_{11}	$05:36:17.84$	$34:06:31.8$	1.1053 ± 0.0007	124	185.267	1.098 ± 0.1033
V_{12}	$05:36:37.89$	$34:03:27.5$	0.8538 ± 0.0004	084	93.789	0.6667 ± 1.0505
V_{13}	$05:36:21.85$	$34:05:40.9$	0.3057 ± 0.0815	076	35.455	0.2857 ± 0.0762
V_{14}	$05:36:43.52$	$34:05:08.8$	0.2665 ± 0.0711	077	13.036	0.2222 ± 0.0775
V_{15}	$05:36:21.81$	$34:05:34.1$	0.3039 ± 0.0810	072	23.669	$0.2041\pm0.0.0105$
V_{16}	$05:35:44.69$	$34:03:03.4$	0.3005 ± 0.0801	087	22.739	0.2941 ± 0.0171
V_{17}	$05:36:38.67$	$34:10:29.8$	$----$	$----$	$---$	$----$
V_{18}	$05:36:17.92$	$34:09:51.1$	$----$	$----$	$---$	$----$

reducing the uncertainty of detected pulsation signal in the scattered data points of light curves of variables. After confirming the pulsation signal of stars, we need a periodogram to estimate the spectral density of a signal during the pulsation signal processing. Now days, the periodogram is computed from the stellar light curves through the implementation of algorithms such as Lomb–Scargle folding [25, 26], Box-fitting Least Squares or "BLS" [27] and Plavchan [28]. Standard and advanced Fourier transform techniques are useful in the analysis of astrophysical time series of very long duration [29] due to their better computing abilities. The Lomb-Scargle algorithm is a variation of the Discrete Fourier Transform (DFT), which decomposes a time series into a linear combination of sinusoidal functions[‡] . This algorithm is implemented by us to detect the pulsation of variables and construct the Fourier-Discrete- periodogram (FDP). In this connection, the 'PERIOD-04' [§] and 'PerSea' [¶] software are used to estimate the period of newly identified variable stars. 'Period04' is dedicated to the statistical analysis of large astronomical time series with gaps and offers tools to extract the individual frequencies from the multi-periodic content. On the other hand, 'PerSea' is based on the analysis of variance (ANOVA) algorithm. In Table 5, the author has listed the resultant estimated period of variables through both software. The phase-folded diagrams of detected regular variables are constructed using the values of the pulsation period as per 'Period04'. The phase-folded light curves of variables of NGC 1960 are shown in Fig. (10a). In these diagrams, the phase values of any variable at time t are defined as decimal part of $(t-JD)/P$, where JD and P represent the Initial Julian Date and Period of the variables. In this connection, the JD value for NGC 1960 is 2455951.11037.

[‡] exoplanetarchive.ipac.caltech.edu/docs/pgram

[§] *www.univie.ac.at/tops/Period04*

[¶] *www.home.umk.pl/ gmac/SAVS/soft.html*

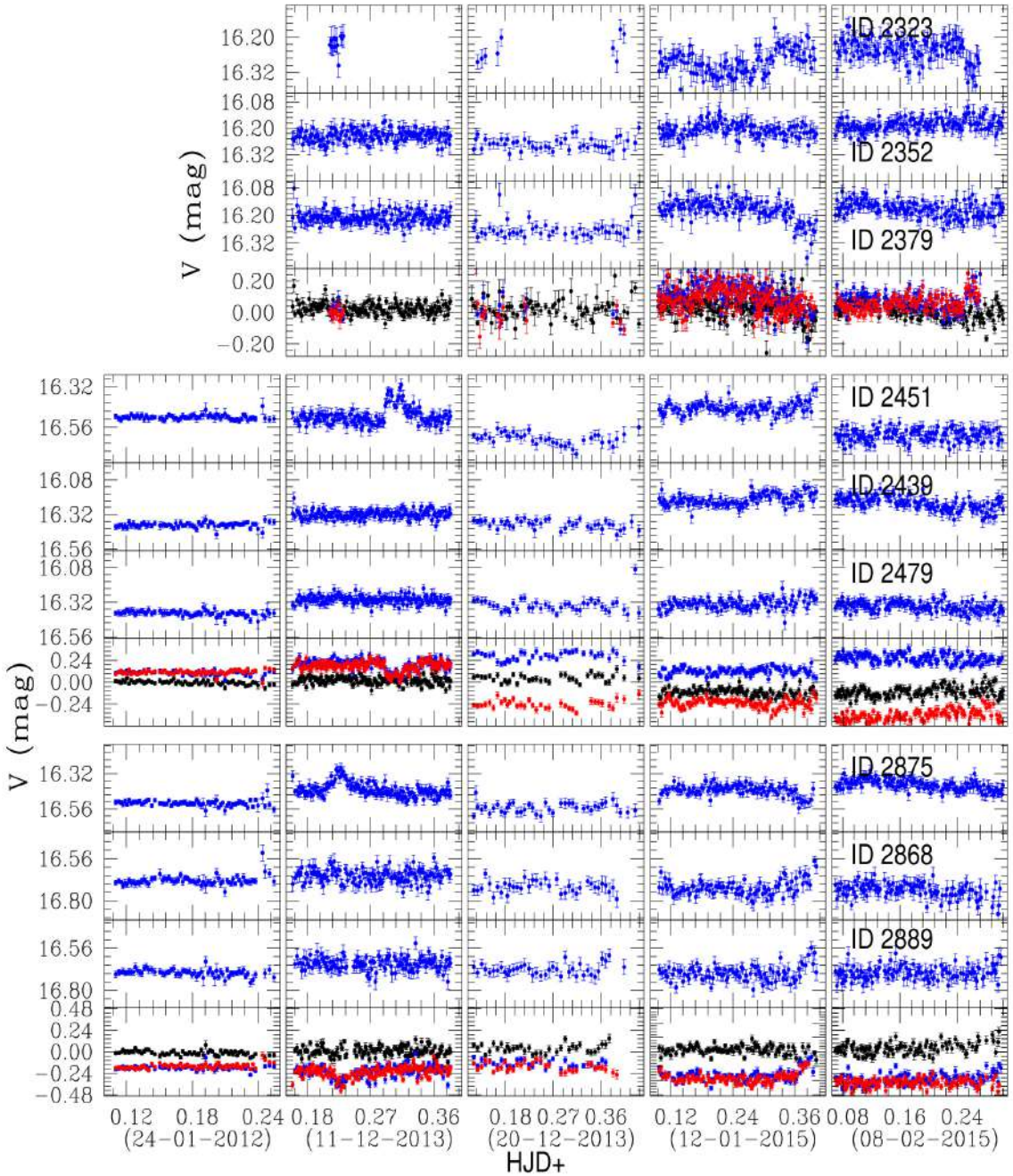

Fig. 9. The panels represent the stellar light curves for star IDs 2323, 2352, 2379, 2439, 2451, 2479, 2868, 2875 and 2889 of cluster NGC 1960. The star IDs 2352 and 2379 are selected comparison stars for Potential variable (V_{16}, Star ID 2323). The star IDs 2439 and 2479 are selected comparison stars for Potential variable (V_{17}, Star ID 2451). The star IDs 2868 and 2889 are selected comparison stars for Potential variable (V_{18}, Star ID 2875).

Table 6. Variable IDs for cluster are listed in first column. Second, third and fourth columns indicate the separation pixel-distances for potential short periodic variable stars and its comparison stars.

Variable ID	$\Delta\ D$ (in pixel)	$\Delta\ D$ (in pixel)	$\Delta\ D$ (in pixel)	SNR	Variable Type
V_1	234.715	373.093	262.214	25.50	$Miscellaneous$
V_2	189.041	509.045	596.828	41.25	$\gamma - Dor$
V_3	448.043	145.154	334.378	17.20	$Miscellaneous$
V_4	231.421	389.344	202.745	07.75	$\gamma - Dor$ (JO20)
V_5	483.260	158.671	444.375	41.33	EB?
V_6	339.534	659.349	792.740	17.25	$Ellipsoidal$
V_7	648.068	916.607	860.138	07.22	$Ellipsoidal$
V_8	145.462	373.379	261.138	14.60	$Rotational$
V_9	643.228	392.418	753.954	23.75	RRC
V_{10}	128.526	925.765	814.031	18.50	$LADS$
V_{11}	132.993	483.626	614.331	24.80	EB
V_{12}	445.491	756.433	312.356	12.00	$Rotational$
V_{13}	554.006	448.464	267.522	19.00	$Miscellaneous$
V_{14}	635.751	813.743	298.683	19.25	$Miscellaneous$
V_{15}	272.533	569.389	297.607	14.40	$LADS$
V_{16}	763.334	599.666	346.557	14.50	$Miscellaneous$
V_{17}	466.030	782.811	320.374	$----$	Irregular
V_{18}	291.715	398.561	640.928	$----$	Irregular

6.1 Smoothness of Phase Diagrams and Change in Amplitude of Pulsation

Here is too much scatter of data points in the original phase diagrams to probe and shape the nature of stellar variability. After applying the moving average procedure, the resultant phase-folded curves of variables are found to be smoother than the original diagrams. As a result, it is concluded that the amplitude of stellar pulsation decreases with the smoothness increment of the phase-folded diagram of variables during the moving average procedure. In the Fig. (10a), the phase diagrams of variables are constructed through the resultant data points as per the average moving procedure. The signal-to-noise ratio (SNR) is defined as $SNR = \frac{A}{e_A}$, where A and e_A are the amplitude of the light curve and the mean estimation error in stellar magnitude, respectively. The SNR values of variable stars are listed in Table 6. In this connection, the phase diagrams for some variable stars (ID 606, ID 1470, ID 1549 and ID 2198) are depicted in Fig. 11 as per period via the 'ANOVA' algorithm.

7 MEAN PROPER MOTION AND MEMBERSHIP ANALYSIS

7.1 Mean Proper Motion of Core region of NGC 1960

A proper motion study of this cluster was done by Sanner et al. (2000) [13], Meurers(1958) [30], Chian & Zho (1966) [31] and Joshi et al. (2020) [32] [JO20 now onward]. Author compared present catalogue with Gaia EDR3 data [33, 34] and found 1579 common stars between them within the studied core region. The distribution of these stars in μ_x-μ_y plane is shown in the Fig. 14. The dark filled circles in the figure are those stars that were used to determine the mean proper-motion of the cluster NGC 1960. These stars were identified after excluding stars located outside 3σ deviation from the mean value of proper motion in both RA and DEC directions. After 3σ iteration processes, the author found 1405 stars that were used to obtain following mean proper motion in RA and DEC direction of the cluster NGC 1960.

$$\bar{\mu_x},\ \bar{\mu_y} = 0.314 \pm 0.026\ mas/yr,$$
$$-2.333 \pm 0.037\ mas/yr$$

JO20 has been estimated the mean proper motion of whole cluster of NGC 1960 in RA and DEC directions as -0.143 ± 0.008 mas yr^{-1} and -3.395 ± 0.008 respectively. Since, JO20 shows a very different selection of cluster members that do not include stars centered around zero pm, therefore their different proper motion values are obvious due to the selection method applied to the stars. Due to the inclusion of field stars, the standard deviation values (σ_α, σ_δ) of stellar proper motions of NGC 1960 are found to be 0.996 and 1.402 in RA and DEC respectively. Using these values, the resultant standard deviation $\sigma = \sqrt{\sigma_\alpha^2 + \sigma_\delta^2}$ is estimated to be 1.734. This standard deviations of the stellar proper motion of cluster NGC 1960 are not compatible with the standard errors of present work as well as the work of JO20. Thus, the different values of proper motions of both studies indicates that the stellar members of this cluster may segregated in inner and outer regions according their proper motion values.

7.2 Kinematic Probabilities

In the present analysis, those stars are consider as kinematic members for each cluster, which are within 3σ limit of the mean proper motion of studied cluster. The proper motion probability is assigned to be 1 for stars that lie within 3σ limit of mean proper motion for the cluster, whereas the proper motion probability is assigned to be 0 for stars with proper motions outside the 3σ limit [35]. By utilizing extracted stellar proper motion from GAIA EDR3 database, new kinematic probabilities of stellar members are computed as $P_{pm} = 1 - \frac{\sqrt{(\mu_\alpha - \bar{\mu_\alpha})^2 + (\mu_\delta - \bar{\mu_\delta})^2}}{3\sigma}$. These values of variable stars of both clusters are listed in sixth column of Table 7.

7.3 Stellar Parallax and Membership

The individual stellar distance of each potential variable star is computed using the parallax information extracted from GAIA EDR3 database and are listed in third column of Table 7. These values are compared with the estimated distance for concerned cluster via CMD analysis. Positional membership of cluster is assigned for those variable stars, whom distance is equal to that of its parent cluster and no positional membership is assigned for other variable stars. A comparative description of the kinematic and positional probabilities for each individual variable stars is given in Section 9.

8 CLUSTER'S PARAMETERS AND LOCATION OF VARIABLE STARS

8.1 Location of Variable Stars of NGC 1960 Compare to ZAMS

By using $(U-B)$ vs $(B-V)$ Two colour Diagram (TCD), Joshi Tyagi, 2015 [5] has been determined reddening, $E(B-V) = 0.23\pm0.02$ mag. JO20 has also computed the reddening, 0.24 ± 0.02 mag, which is close to the previous one. In the present work, the location of variable stars of NGC 1960 is shown in $(U-B)$ vs $(B-V)$ TCD along-with Zero-Age-Main-Sequence (ZAMS) as shown in Fig. 15. A ZAMS star has minimum radius, maximum mass (for single star evolution), bluest colour (or hottest effective temperature), and central core possesses its peak H/He [36]. After deep inspection of TCD and GAIA database for cluster, author has been drawn following facts:

(1)- Variable stars V_1, V_2, V_3. V_4 are found to be ZAMS stars and have close brightness to each other in V-band. The locations of V_1, V_2 and V_4 at the near of bump in $(U-B)$ vs $(B-V)$ TCD, whereas the location of V_3 is found to be far away these stars. This facts leads different class of V_3.

(2)- Variable stars V_8, V_{12}, V_{13}, V_{14} and V_{16} are belong to ZAMS of cluster. Variable stars V_8 and V_{12} are member of cluster 1960 and may poses the character of same class of variable stars. Variable stars V_{13}, V_{14} and V_{16} are field stars leading to the fact that field stars are also located in just main sequence of cluster.

(3)- Variable stars V_6, V_{10}, V_{11}, V_{15}, V_{17} and V_{18} do not belong to main sequence of cluster and have a confirm membership of cluster.
(4)- Variable stars V_5, V_7, and V_9 neither belong to main sequence of cluster nor are members of cluster.

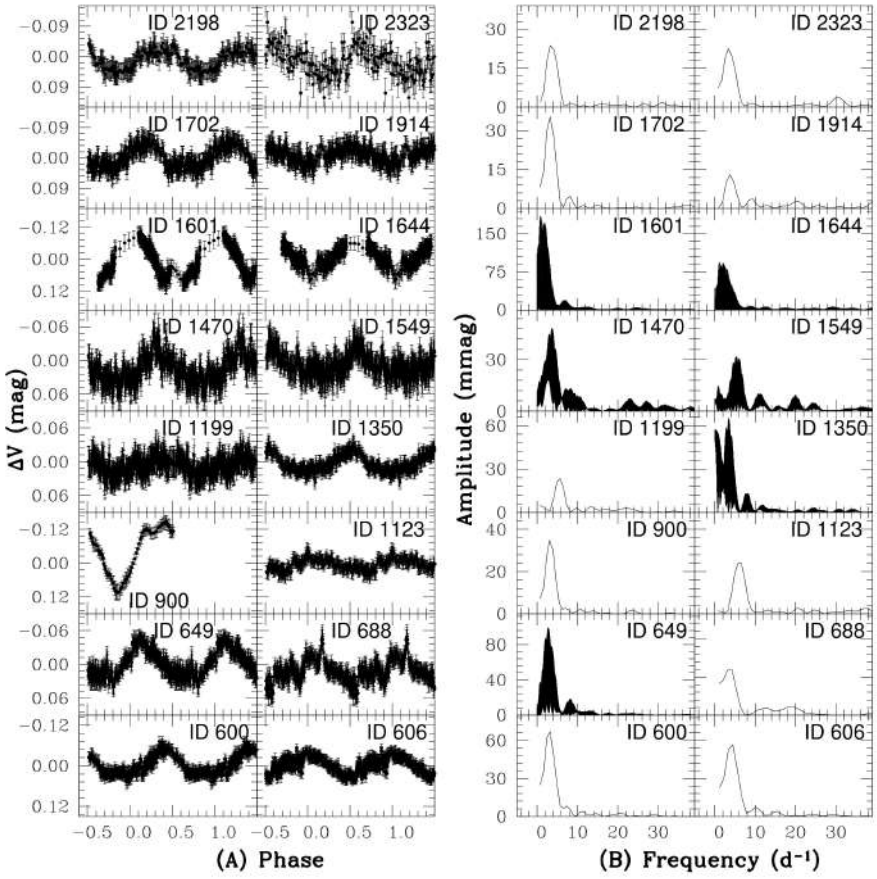

Fig. 10. The left panels represent the phase-folded-diagrams of identified variable stars within the cluster NGC 1960, whereas their corresponding DFT represent in the right panels.

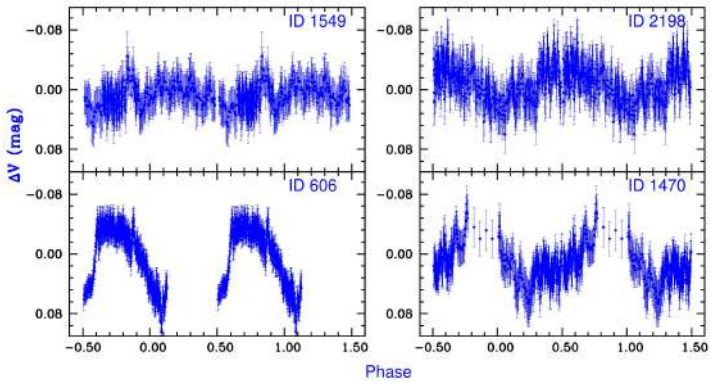

Fig. 11. The panels represent the phase-folded-diagrams of variable stars (ID 606, ID 1470, ID 1549 and ID 2198) of cluster NGC 1960 as per period via 'ANOVA' algorithm.

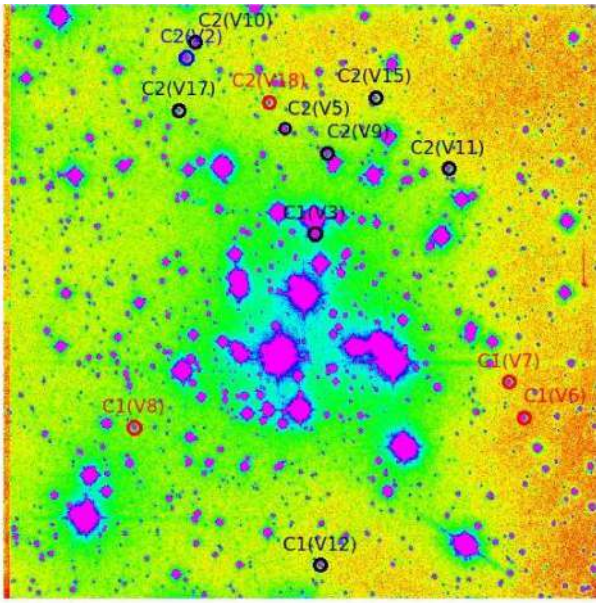

Fig. 12. The finding chart for selected comparison stars within cluster NGC 1960. Identified standard stars are marked by red open circles and they have almost constant brightness/flux during observations. Black open circles represent those long periodic variable stars, for which approximate flux is found for a particular night of observation. However, the value of magnitude is varying nigh to night.

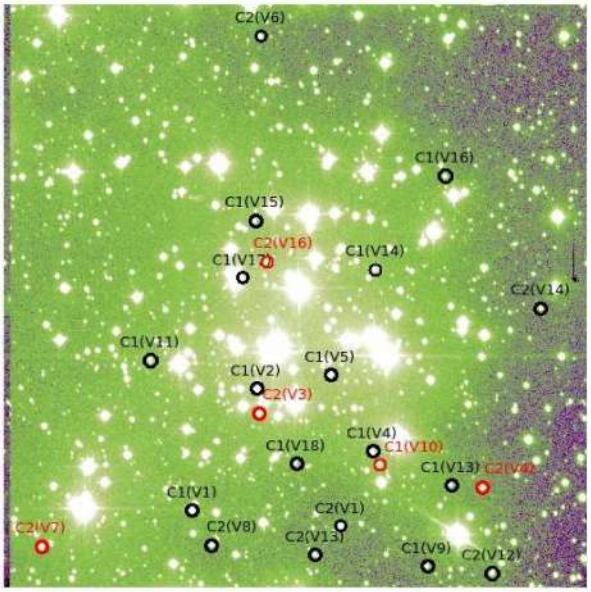

Fig. 13. The finding chart for selected comparison stars within cluster NGC 1960. Red open circles represent those Long term variable stars, for which variation in brightness is also found as daily basis. Black open circles are depicted stars that have irregular flux variation in their light curves as extracted through absolute photometry.

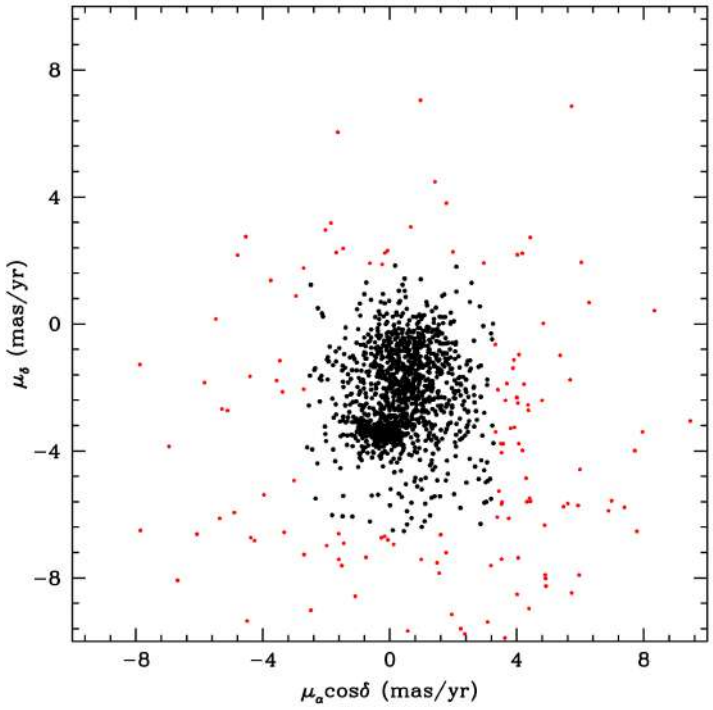

Fig. 14. The distribution of proper motion of stars present in the cluster region. The large black points represent those stars which are used to determine the mean proper motion of the cluster

Table 7. Prallax and distance values of studied variable stars are listed in second and third columns respectively. The stelar proper motion values of R.A. and DEC deirection are given in fourth and fifth columns respectively. The estimated kinematic probabilities of variables are listed in sixth column.

Variable ID	Parallax (mas)	Distance (kpc)	Proper Motion in RA (δ)	Proper Motion in DEC (μ)	kinematic Pro. (Old)	kinematic Pro. (GAIA)
V_1	0.8858±0.0188	1.129±0.024	−0.204±0.023	−3.406±0.016	0.40	0.771
V_2	0.8430±0.0180	1.186±0.025	−0.011±0.023	−3.506±0.017	0.35	0.766
V_3	2.9243±0.0228	0.342±0.003	−3.018±0.027	−4.932±0.019	0.06	0.188
V_4	0.8382±0.0194	1.193±0.027	−0.432±0.024	−3.219±0.017	0.99	0.777
V_5	0.2889±0.0255	3.461±0.305	0.675±0.028	−2.292±0.021	0.05	0.930
V_6	0.8543±0.0254	1.171±0.035	−0.209±0.034	−3.440±0.023	0.81	0.765
V_7	0.1985±0.0275	5.038±0.698	0.113±0.027	−1.594±0.021	0.00	0.853
V_8	0.8206±0.0350	1.219±0.052	−0.042±0.040	−3.525±0.026	0.79	0.761
V_9	0.4966±0.0857	2.014±0.348	0.010±0.097	−3.579±0.072	0.91	0.753
V_{10}	0.8022±0.0309	1.246±0.048	−0.244±0.036	−3.276±0.027	0.04	0.789
V_{11}	0.8130±0.0350	1.230±0.053	−0.401±0.043	−3.543±0.030	0.94	0.730
V_{12}	0.9063±0.0400	1.103±0.049	−0.059±0.049	−3.355±0.035	0.00	0.791
V_{13}	0.4407±0.0366	2.269±0.188	0.723±0.041	−3.327±0.029	0.00	0.793
V_{14}	0.0995±0.1441	10.050±14.555	0.692±0.159	−2.518±0.128	0.99	0.919
V_{15}	0.9037±0.0496	1.106±0.061	−0.331±0.055	−3.593±0.037	0.00	0.728
V_{16}	1.1574±0.0478	0.864±0.036	4.521±0.057	−1.697±0.038	0.93	0.182
V_{17}	0.9037±0.0448	1.107±0.055	−0.178±0.055	−3.418±0.040	0.52	0.771
V_{18}	0.8396±0.0460	1.191±0.065	−0.246±0.054	−3.425±0.039	0.95	0.764

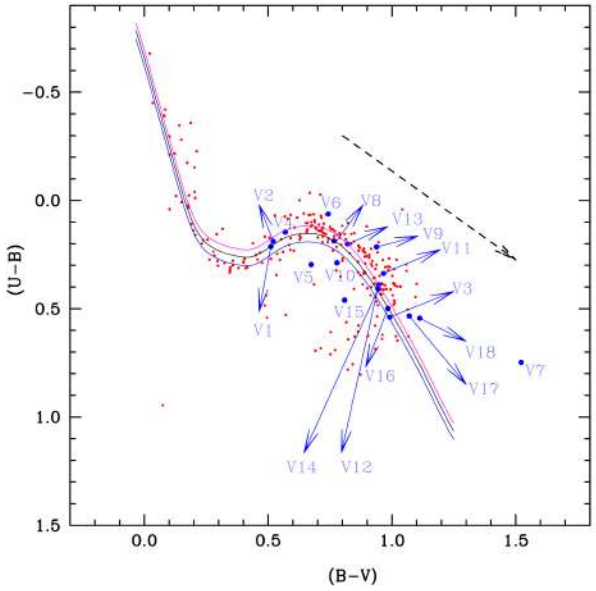

Fig. 15. $(B-V)$ **vs** $(U-B)$ **colour-colour diagram for the MPMs in the field of cluster NGC 1960 as per Joshi & Tyagi (2015). For clarity, variable stars of NGC 1960 are represented by blue dots. The dotted black arrow shows a slope of normal reddening vector** $E(U-B)/E(B-V)$**=0.72. The solid black line shows the best fit taken in account of 0.23 and 0.17 mag shift in** $(B-V)$ **and** $(U-B)$**, respectively while pink and blue lines represent an error of** $\pm$**0.15 in the reddening vector respectively.**

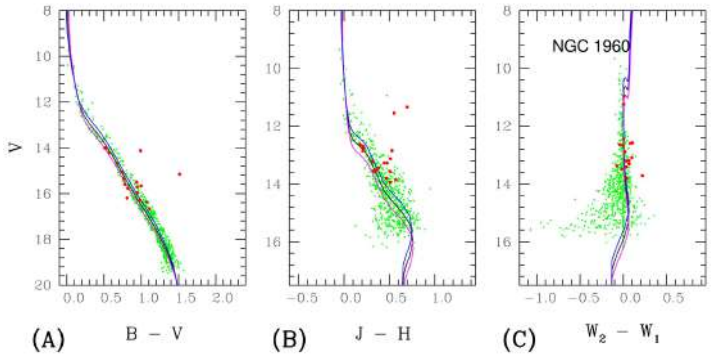

Fig. 16. The panels of this figure represent CMDs for NGC 1960. The red dots on each panel represent the variable stars as identified by us through the time series photometric data while green dots represent the probable members of the studied clusters as extracted from the work of Joshi & Tyagi (2015) and Joshi & Tyagi (2015b). The black solid lines represent the best fitted theoretical isochrones as given in the previous studies. In the panel 16 (A), there are no variable stars situated near the turn-off region of NGC 1960 due to selected magnitude range ($13.17\pm0.30\ mag$ **to** $16.61\pm0.30\ mag$**) in V-band.**

8.2 CMDs Analysis for NGC 1960

The log-age of this cluster has been reported by Kharchenko et al. (2004) [11], Joshi & Tyagi (2015) [5] and JO20 as 7.62 (yr), 7.35 (yr) and 7.44 (yr), respectively. Joshi & Tyagi (2015) [5] have shown the most probable members (MPMs) in $(B-V)$ vs V Colour Magnitude Diagram (CMD) by comprehensive analysis of photometric, kinematic and spatial probabilistic criteria. These MPMs are found along with MS of NGC 1960 and is also well aligned with a well fitted theoretical isochrone as depicted in the panels of Fig. 16. The pink line of each CMD represents the well fitted theoretical isochrone as computed by Joshi & Tyagi (2015) [5]. In the $(J-H)$ vs H CMD, author did not find stellar alignment by MPMs along with theoretical isochrone for H-magnitude range of 12.5-13.2 mag as shown in Fig. (16B). Thus, an improvement is needed in estimation of distance-modulus. Author overplot Marigo's theoretical isochrones on the CMDs by varying the distance modulus and age simultaneously by keeping reddening $E(B-V)=0.23$ mag. From the best visual isochrone fit to the varying age and distance combinations, author obtained a distance modulus $(V-M_V) = 11.05\pm0.0.30$ mag and $log(Age) = 7.35\pm0.05$ (yr) for cluster NGC 1960. Employing the correction for the reddening and assuming a normal reddening law, this corresponds to a true distance modulus $(m-M)_0 = 10.34\pm0.30$ mag or a distance of $1.169\pm0.173\ kpc$ for the cluster. This distance is close to that of $1.17\pm0.06\ kpc$ as estimated by JO20 via a mean parallax, $0.86\pm0.05\ mas$, for probable cluster members of NGC 1960 (For this purpose, parallax values were extracted by JO20 from GAIA database). The computed value of distance modulus is used to identify the true member of cluster according to retrieved value of distance/parallax value of individual star.

The best fitted theoretical isochrones in each CMD is represented by black line and identified variable stars are depicted by red dots. Variable stars V_3 and V_7 show colour excess in near-infrared bands, however these stars also found along-with the theoretical isochrone in $W_2-W_1\ vs\ W_1$ CMD as depicted in Fig. (16C).

8.3 Range of Instability Strip for Searching Variable Stars

The instability strip is a narrow, almost vertical region in HR diagram, which includes many different types of variable stars. Most stars more massive than Sun enter the instability and become variable at least once after leaving the main sequence (MS) [‖]. This strip intersect the MS in the region of A and F stars (masses 1-2 $M_\odot$) of studied clusters and extends to G and early K bright super-giants. The common area of instability strip and MS of star cluster NGC 1960 seems to be important region (includes A and F stars) for understanding the cluster dynamics through the stellar variability and vice-versa. To determine the location of the A/F type stars in the colour-magnitude diagram, distance modulus, $(V-M_V) = 11.05\pm0.30\ mag$, was applied to obtain the V-magnitudes. In this connection, the upper and lower limit of region, have A and F stars, are found to be $13.17\pm0.30\ mag$ of $V-band$ and $16.61\pm0.30\ mag$ of $V-band$, respectively and prescribed intercepted region also least affected by the brighter stars and their neighbourhood. Consequently, author is carried out time series analysis for finding stellar variability within this magnitude-range. A total of eighteen variables of NGC 1960 have been identified in this magnitude-range. In the present case of NGC 1960, the author did not perform any analysis to search variable stars in near the turn-off region and region of faint stars.

9 CLASSIFICATION OF DETECTED VARIABLE STARS WITHIN NGC 1960

In this paper, eighteen variables were detected in the field of view of NGC 1960, four of them are common with the four variable stars of JO20. According to the behavior of the light curves and the period analysis, the identified variable stars were classified as given below,

9.1 $\gamma-Doradus$ Variables

The light curves of regular variable stars are repeating with a constant value of time (i.e. its period). A multiperiodic stars with g-mode pulsation is called a $\gamma-Doradus$. These are typically young, early F- or late A-type main stars with periods in the range of about $0.3-3\ d$ and brightness fluctuation $\sim 0.1\ mag$ [37].

9.1.1 Star ID 606 (V_2), 616 and 626 of NGC 1960)

In the case of variable star ID 606, star IDs 616 (5^h : 36^m : 26.45^s, $+34^0$: $07^{'}$: $39.3^{"}$) and ID 624 (5^h :

[‖] *astronomy.swin.edu.au/cosmos/I/Instability Strips*

$35^m : 50.83^s$, $+34^0 : 06^{'} : 03.6^{"}$) are selected for comparing their light curves with it. JO20 is assigned ID 606 as a cluster member $\delta - Scuti$ variable star with period $0.27632 \pm 0.00008\ d$ and is denoted by V_{35} in their analysis. In the present work, its period is computed as $0.2246 \pm 0.0599\ d$ and $0.6250 \pm 0.0274\ d$ by the codes of 'PERIOD04' and 'PerSea', respectively. Both computed vales are far from the length of data string, and shows a characteristic of multi-periodicity. Since its light curves in Fig. 4 shows no indication of period value less than 7.6 hours, therefore its period value appears to be more accurate via Anova analysis. Thus, Star ID 606 is detected as a $\gamma - Doradus$ variable star instead of $\delta - Scuti$. Its kinematic probability makes it as the most likely member of cluster.

The light curves of ID 616 are showing irregular flux variations, whereas the light curves of ID 624 have characteristics of long periodic type variable stars. Almost constant magnitude was found for ID 624 during 7-8 hours of observations.

9.2 RR Lyre Stars

Over 80 $\%$ of all variables known in globular clusters are RR Lyre stars [38]. One d-type RR Lyre variable star in the open cluster NGC 2141 has been reported by Luo (2015) [39]. RR Lyrae variables do not follow a strict period-luminosity relationship at visual wavelengths, although they do in the infrared K-band [40].

9.2.1 Star IDs 1431, 1470 (V_9) and 1484 of NGC 1960

The variable star V_9 is assigned as a rotational variable star, main sequence star and cluster member by JO20 and marked by V_{48} in their analysis. Its period is computed to be $0.2667 \pm 0.0006\ d$ and $0.4629 \pm 0.0399\ d$ by the codes of 'PERIOD04' and 'PerSea' respectively. These codes clearly provide two distinct values of period. It seems that computed period $0.2667 \pm 0.0006\ d$ (as per 'PERIOD04' code)is an average length of data strings in 2013 and 2015, whereas period value $0.4629 \pm 0.0399\ d$ (as per 'PerSea' code) is cross matched with period 0.47483 ± 0.00023 as estimated by JO20. Its location in $(U-B)\ vs\ (V-B)$ TCD indicates that it does not meet the criteria of ZAMS within errors as depicted in Fig. 15. Its distance is $2.014 \pm 0.348\ kpc$ as per GAIA database, which is very far from the cluster NGC1960. Thus, the variable star V_9 neither a main sequence star nor a member of cluster NGC 1960. Its highest probabilistic values are just coincidence with the members of cluster. Since, its characteristics do not match well with those of a rotational type variable star, therefore author switched off its previous classification as did by JO20.

The slowly descending and quickly ascending nature of its phase-folded curve indicates that variable star V_9 is a RR Lyre star.

Star IDs 1431 ($5^h : 36^m : 45.65^s$, $+34^0 : 11^{'} : 25.0^{''}$) and 1484 ($5^h : 36^m : 00.93^s$, $+34^0 : 09^{'} : 07.7^{''}$) have been selected comparison stars for the variable star V_9. Their locations in Figs. 13 and12 are marked by C1(V9) and C2(V9) respectively. By visual inspection, author found that these comparison stars are far from the variable star V_9. The comparative light curves of star IDs 1431 and ID 1484 show a constant magnitude difference during entire observational session. According to GAIA database, the parallax values for Star IDs 1431 and 1484 are $0.6473\ mas$ and $0.2435\ mas$, respectively. The colour-difference $(B-V)_0$ for both comparison stars is greater than 1.0 mag. Such pair of comparison stars is not possible for any given variable star as per differential photomery. Consequently, magnitude variation of stars is free from stellar distance and colour-difference in absolute/ standard photometry. Although, the author found some amount of magnitude variation for both comparison stars and this seems instrumental effect in nature.

9.3 Eclipsing Binaries Type Variable Stars

Eclipsing binaries are conveniently classified into two main groups: detached system or semidetached [41]. Spherical or slightly ellipsoidal components are found in detached system (Algol type, EA), whereas tidally distorted stars are present in semidetached system (β Lyre System, EB). The light remains nearly constant between eclipses of EA systems. Between eclipses, a continuous change of the combined brightness is found for EB system, making it impossibility to assign the exact times of onset and end of eclipses. Stars with planets can also show flux variations if associated planets for any star pass between Earth and the star.

9.3.1 Star IDs 900 (V_5), 902 and 904 of NGC 1960

Star ID 902 is marked by V_{55} by JO20 and assigned as a field star in their analysis. Furthermore, they

found a minima in its phase curve with an amplitude of $218\ mmag$. In the case of $V_5(ID900)$ at Fig. 5, the different light curve show a partial eclipse and part of an eclipse. The full eclipse is detected in its light curve of 20 December 2013 and a portion of eclipse also detected in its light curve of 12 January 2015. The gap of both detected eclipses is 01 year 23 days 3 hours. The other nights show a constant data string. This is a classical light curve of an eclipsing binary due the rounded shape. Author found only one full minima in its light curves with amplitude of $248\ mmag$ and it is close to estimated amplitude by JO20. In the present work, the light curves of variable star V_5 are shown in Fig. 5. The time of eclipse is computed through the codes of 'PERIOD04' and 'PerSea' to be $0.3182{\pm}0.0848\ d$ and $0.2857{\pm}0.0454\ d$ respectively, which are not true periods. Both of these values are equivalent to the data strings, in which eclipse has detected. After visual inspection of light curves of this variable, estimated time of eclipse is approximately $0.216{\pm}0.018\ d$. Its distance is $3.461{\pm}0.305\ kpc$ and lies far away from the cluster periphery. Thus, it is a background for having field star in the field of cluster NGC 1960.

Light curves of Star IDs 902 ($5^h : 36^m : 25.02^s,\ 34^o : 09^{'} : 17.5^{''}$) and 904 ($5^h : 35^m : 58.41^s,\ 34^o : 08^{'} : 11.8^{''}$) have been selected for comparative analysis with those of the variable star V_9. Both comparison stars have nearby colour, $((B-V)_0)$, value with variable star V_9. The light curves of Star ID 904 has short periodic variation with low amplitude, whereas light curves of star ID 902 has irregular variation of brightness. Since, brightness fluctuation in their comparative light curves is almost constant, therefore, fluctuation of their light curves is a result of instrumental errors in nature.

9.3.2 Star IDs 1576, 1601 (V_{11}), 1613 of NGC 1960

Based on the 'PERIOD04' and 'PerSea' codes analysis, author obtained period values for V_{11} as $1.1053{\pm}0.0007\ d$ and $1.0980{\pm}0.1033\ d$, respectively. Its distance from us is $1.230{\pm}0.053\ kpc$ and its kinematic probability of membership in cluster is 0.73 as per proper motion via GAIA database. Thus, variable star V_{11} is a member of cluster. It can be easily seen in its light curves, which are depicted in Fig. 7 that have short periodic variations superimposed with its principal period. The continuous change in brightness makes it difficult to assign the exact time of onset and end of eclipses of companion stars, and its phase-folded diagram shows the superimposed character of both eclipses as depicted in Fig. 10. Hence, this star is classified as a semidetached eclipsing binary (EB) type variable star.

The pattern of brightness variation in light curves for star ID 1576 ($5^h : 36^m : 23.38^s,\ 34^o : 05^{'} : 18.1^{''}$) is similar to that of variable star V_{11} as depicted in Fig. 7. As a result, author concluded that star ID 1576 is also an EB star with low amplitude. During the observational session of each night, light curves of star ID 1613 ($5^h : 36^m : 02.64^s,\ 34^o : 11^{'} : 46.0^{''}$) shows an incremental slop over time with least inclination. In this connection, the fluctuation of its light curves is seem to be instrumental errors in nature.

9.4 Ellipsoidal Variable Stars

In the periodogram of an ellipsoidal binary, sharp peaks are found at the fundamental frequency and its harmonics. Usually only the first harmonic is visible and the amplitude of fundamental frequency is less than first harmonic in some cases. As a consequence of differences in harmonic content, the shapes of the light curves can be very different [41]. These stars are close binary system and tidally distorted components. There are no eclipses in these variables due to the low inclination of the orbital axis, but the changing aspect towards us causes a change in brightness. Such brightness variation are a combination of tidal distortion, reflection and beaming. The period of the reflection and beaming contributions have the same period as the orbital period whereas the ellipsoidal effect has half the orbital period [41].

9.4.1 Star IDs 1123 (V_6), 1124 and 1130 of NGC 1960

Based on the codes of 'PERIOD04' and 'PerSea', the period of V_6 is found to be $0.1528{\pm}0.0194\ d$ and $0.1538{\pm}0.0369\ d$, respectively. Its distance ($1.171{\pm}0.035\ kpc$) and kinematic probabilistic value (0.765) indicate that it is a member of cluster. Since, non-sinusoidal variation is found in its phase folded light curve, therefore it has the characteristics of ellipsoidal type variable star. However, a comprehensive analysis of its light curves during whole observational session indicates that it is an irregular type variable. As a result, it is classified as an irregular variable with character of ellipsoidal.

Star ID 1124 ($5^h:36^m:28.92^s,\ 34^o:13^{'}:23.2^{''}$) has been selected as first comparison star for the variable star V_6. It shows almost constant magnitude with time as shown in Fig. 5. Thus, it is classified as stable star in the direction of cluster NGC 1960 and its physical location is marked by C1(V6) in Fig. 12.

Similarly, star ID 1130 ($5^h:35^m:48.78^s,\ 34^o:07^{'}:46.3^{''}$) has been selected as second comparison star for the variable star V_6. This star is classified as an irregular type variable by JO20 and denoted by V_{70} in their analysis. After visual inspection of its light curves in Fig. 5, the author also confirms its character of irregular type variable star.

9.4.2 Star ID 1197, 1199 (V_7), 1204 of NGC 1960

The value of period for variable star V_7 is computed to be $0.1747\pm0.0254\ d$ and $0.1695\pm0.0154\ d$ using the codes of 'PERIOD04' and 'PerSea' respectively. In the present work, its kinematic probabilistic value is estimated to be 0.853 as per proper motion values via GAIA database. Unfortunately, its distance ($5.038\pm0.698\ kpc$) does not confirm its membership in the cluster, NGC 1960. Due to a non-sinusoidal variation of brightness in its light curves, variable star V_7 is classified as an ellipsoidal type variable star. Its position in $(U-B)$ vs $(B-V)$ TCD confirms its red character of colour.

Its First Comparison star, ID 1197 ($5^h:36^m:25.21^s,\ 34^o:13^{'}:04.1^{''}$), shows nearly constant magnitude during observational session as depicted in Fig. 6. As a result, it is a stable star and its position is marked by C1(V7) in Fig. 12.

Similarly, light curves of its second comparison star, ID 1204 ($5^h:36^m:43.20^s,\ 34^o:02^{'}:51.6^{''}$), show the character of irregular type variable star.

9.5 Rotational Variable

Stellar rotation and magnetic activity are normally associated with a main-sequence star of G or later spectral type [32]. The amplitude of pulsation of these stars is usually less than 0.1 mag. Thus, these stars are characterized by small amplitude, and red in colour $(B-V)_0 > 0.5\,mag$. The periods of rotational variable stars can vary widely due to its tied with the own rotation of the stars.

9.5.1 Star IDs 1345, 1348 and 1350 (V_8) of NGC 1960

Using the codes of 'PERIOD04' and 'PerSea', the period values for V_8 are estimated to be $0.2864\pm0.0007\ d$ and $0.2857\pm0.0947\ d$ respectively. The lengths of individual data strings are $0.3167\ d$ and $0.3000\ d$ on date 20/12/2013 and 12/01/2015, respectively and these values are greater than $0.2864\pm0.0007\ d$. Its character of variability is confirmed in individual data strings. It is located at $1.219\pm0.052\ kpc$ from us and this value is close to the distance of cluster. In this connection, its kinematic probabilistic value for cluster membership is 0.761 leading member of studied cluster. It is red in colour, $(B-V)_0 = 0.766\ mag$. Its location in $(U-B)$ vs $(B-V)$ TCD is found with ZAMS as shown in Fig. 15. All the above characters make it a rotational type variable star.

The light curves of star IDs 1348 ($5^h:36^m:29.70^s,\ 34^o:04^{'}:53.6^{''}$) and 1345 ($5^h:36^m:43.22^s,\ 34^o:06^{'}:38.6^{''}$) are shown in Fig. 6. Almost constant magnitude in light curves of star ID 138 make it a stable star, whereas star ID 1345 has a character of long periodic type variable stars.

9.5.2 Star IDs 1644 (V_{12}), 1732 and 1734 of NGC 1960

Based on 'PERIOD04' and 'PerSea' code analysis, obtained values of period for variable star V_{12} are $0.8538\pm0.0004\ d$ and 0.6667 ± 1.0505 respectively. In $(U-B)$ vs $(B-V)$ TCD, it is located just on the main sequence. It has a red character in colour, $(B-V)_0 = 0.946\ mag$. As per GAIA database, its distance is found to be $1.103\pm0.049\ kpc$ with a kinematic probability 0.791. Thus, it is a member of cluster, NGC 1960, along with the main sequence. The amplitude of this variable is found to be $94\ mmag$ via code of PERIOD04. In this connection, it is classified as a rotational type variable star.

The light curves of star ID 1732 ($5^h:36^m:44.29^s,\ 34^o:08^{'}:55.9^{''}$) shows short term variability with low amplitude, which appears to be instrumental error in nature. Beside this, it is approximately constant magnitude during observation. Other hand, the light

curves of star ID 1734 ($5^h : 36^m : 46.46^s,\ 34^o : 12^{'} : 51.3^{''}$) show a incremental slop of low inclination over observation as shown in Fig. 7.

9.6 Low Amplitude Delta Scuti Variable

Low-amplitude delta Scuti stars (LADS) have pulsation with smaller amplitudes. The low-amplitude stars can be pre-main, main or post-main sequence stars, and can be either multiperiodic or monoperiodic** .

9.6.1 Star IDs 1549 (V_{10}), 1553 and 1569 of NGC 1960

The value of distance ($1.246\pm0.048\ kpc$) and kinematic probability (0.789) of variable star V_{10} confirm membership of the cluster. Its location in $(U-B)$ vs $(B-V)$ TCD makes it as a post-main sequence star. Author analyzed the frequencies of variable star V_{10} with Fourier and variance analysis using codes of 'PERIOD04' and 'PerSea'. After these analyses, the computed period is found to be $P_1 = 0.1886\pm0.0003$ and $P_2 = 0.2404\pm0.0226$, respectively, leading to $P_1/P_2 = 0.78$. The amplitude of pulsation is $74\ mmmag$ as per Lomb-Scargle algorithm. So it is suggested that V_{10} is a multi-periodic $\delta - Scuti$ star with low amplitude.

Due to almost constant difference of stellar magnitudes in the comparative light curves of Star IDs 1553 ($5^h : 36^m : 34.70^s,\ 34^o : 10^{'} : 22.7^{''}$) and 1569 ($5^h : 35^m : 49.15^s,\ 34^o : 06^{'} : 15.1^{''}$), their magnitude variation for one observational night is a result of instrumental transformation. However, the light curves of star ID 1569 show a character of long-term variability as shown in Fig. 7.

9.6.2 Star IDs 2195, 2198 (V_{15}) and 2222 of NGC 1960

The variable star (V_{15}) is a member of cluster due to its distance ($1.106\pm0.061\ kpc$) and kinematic probability (0.728). It is also found to be a post-main sequence star according to its position in $(U-B)$ vs $(B-V)$ TCD. The values of period for variable star V_{15} are computed using the codes of 'PERIOD04' and 'PerSea' to be $0.3039\pm0.0810\ d$ and $0.2041\pm0.0105\ d$ using the codes of 'PERIOD04' and 'PerSea' respectively. Since, the computed value of $0.3039\pm0.0810\ d$ (as per PERIOD04) is close to the length of individual data string therefore, it is not a true period for variable star V_{15}. However, it leads to a ratio of $\nu_1 : \nu_2 = 3 : 2$. As per Lomb-Scargle algorithm, the pulsation amplitude for this star is $72\ mmag$. Thus, it appears to be low amplitude $\delta - Scuti$ type variable star.

The light curves of star IDs 2195 ($5^h : 36^m : 08.50^s,\ 34^o : 07^{'} : 37.9^{''}$) and 2222 ($5^h : 35^m : 55.14^s,\ 34^o : 10^{'} : 10.8^{''}$) show no sign of reasonable variability and their comparative light curves show almost constant difference for their magnitudes as shown in Fig. 8.

9.7 Irregular and miscellaneous Variable Stars

Mira variables have less regular light curves with large amplitudes of several orders of magnitudes, while semi-regular variables have less regular with smaller amplitudes [42]. In this connection, the amplitudes of light curves of irregular variable stars do not occur after a fixed time interval and shape of their light curves has been found to be in an uncertain pattern. Consequently, the variations in brightness show no regular periodicity in an irregular type variable star. Such stars are divided into eruptive and irregular pulsating variable stars. The variation of brightness of an eruptive variable star happens due to violent processes and flares occurring in its chromosphere ana coronae. Eruptive variable stars are found near the main sequence.

9.7.1 Star IDs 635, 645 and 649 (V_3) of NGC 1960

The codes of 'PERIOD04' and 'PerSea' give its period value as $0.3598\pm0.0001\ d$ and $0.4000\pm0.2086\ d$ respectively. These values are close to length of individual data strings in 2015. The length of data string ($0.3598\pm0.0001\ d$) of variable star V_3 lead to a peculiar phase-fold diagram with slowly descending and quick ascending branches as similar to the $RR\ Lyre$ variable stars. In this connection, its least kinematic probabilistic value and distance indicate that it is not a member of cluster NGC 1960. However, its position in $(B-V)\ vs\ V$ CMD and $(U-B)\ vs\ (V-B)$ TCD is just on the main sequence. Its position in $(U-B)\ vs\ (V-B)$ TCD is found to be far away

** $aavso.org/vsots_delsct$

from the group of identified $\delta - Scuti$ variable stars. In addition, length of individual data strings is too long for normal $\delta\ Scuti$ star. Under these circumstance, it is impossible to classify its variability type. As a result, it is listed as miscellaneous variable star in present analysis.

In the case of this variable star, Star IDs 635 ($5^h : 36^m : 09.47^s, +34^0 : 08^{'} : 51.2^{''}$) and 645 ($5^h : 36^m : 29.11^s, +34^0 : 07^{'} : 42.2^{''}$) are selected for the comparative analysis. Star ID 635 is assigned as a $\gamma - Dor$ variable star by JO20. In this connection, author found that light curves of Star ID 635 show characteristic similarities to that of star ID 624. Similarly, light curves of star IDs 616 and 645 have similar characteristics. Thus, the nature of the light curves of star IDs 616, 624, 635 and 645 are either uncertain in nature or have some kind of irregular variability.

9.7.2 Star IDs 1701, 1702 (V_{13}) and 1732 of NGC 1960

The distance for variable star, V_{13}, is $2.269\pm0.188\ kpc$ via proper motion values as extracted from the GAIA database. Its kinematic probability coincides with that of the member of cluster. Its light curves show a non-sinusoidal variation of brightness as shown in Fig. 8. As per codes of 'PERIOD04' and 'PerSea', the estimated values of period for variable star V_{13} are $0.3057\pm0.0815\ d$ and $0.2857\pm0.0762\ d$, respectively. Both values are similar to time length of individual data string during 2015, which is a misleading period. Phase curve via $0.3057\pm0.0815\ d$ poses a fine curve as shown in Fig. 10 for ID 1702. This period coincidentally seems close to length of the data string. As a result, it has been classified as miscellaneous type variable star due to lack of continuous data.
Star IDs 1701 ($5^h : 36^m : 36.95^s, 34^o : 11^{'} : 57.0^{''}$) and 1732 ($5^h : 36^m : 44.29^s, 34^o : 08^{'} : 55.9^{''}$) are selected for comparative analysis and their positions are marked by C1(V13) and C2(V13) in Fig. 13. After visual inspection of light curves of both comparison stars in Fig. 8, author found a constant magnitude difference between the both comparison stars. As a result, it is concluded that character of irregular type variability of both stars is an instrumental effect in nature.

9.7.3 Star IDs 1893, 1914 (V_{14}) and 1915 of NGC 1960

Using codes of 'PERIOD04' and 'PerSea', estimated value of period for variable star V_{14} is computed to be $0.2665\pm0.0711\ d$ and $0.2222\pm0.0775\ d$, respectively. Both computed values are close to average length of data strings. It is located at $10.050\pm14.555\ kpc$ as per extracted parallax from GAIA database, which is highly uncertain. A high kinematic probability is not enough to assign membership status to a star. Its location in $(U-B)$ vs $(B-V)$ TCD is just on the main sequence. Its depicted light curves in Fig. 8 show a non-sinusoidal variation of brightness. The pixel coordinates and light curves of this variable star suggested that its flux is affected by instrumental errors leads an uncertainty for computing periods as well as analysis of its light curve. As a result, it is classified as miscellaneous type variable star.
In Fig. 13, the star IDs 1893 ($5^h : 36^m : 13.78^s, 34^o : 10^{'} : 18.2^{''}$) and 1915 ($5^h : 36^m : 18.07^s, 34^o : 13^{'} : 58.4^{''}$) are marked by C1(V14) and C2(V14) respectively. The light curves of Star ID 1893 show the character of a long periodic variables, whereas Light curves of star ID 1915 are almost constant for some night of observation and have incremental slope with low inclination for other nights of observation.

9.7.4 Star IDs 2323 (V_{16}), 2352 and 2379 of NGC 1960

Using codes of 'PERIOD04' and 'PerSea', the estimated values of period for V_{16} are $0.3005\pm0.0801\ d$ and $0.2941\pm0.0171\ d$ respectively. Its phase curve via $0.3005\pm0.0801\ d$ posses a character of asymmetrical magnitude variation with increasing rapidly and decreasing slowly. The said phase curve seems to be distorted in nature as depicted in Fig. 10. Both periods were found close to length of individual data-string in 2015, therefore both are not true period for variable star. Such misleading period produces distortion in phase diagram compared to their light curves. Its distance is $0.864\pm0.036\ kpc$ according to parallax value as extracted from GAIA database and it is close to us with respect to the cluster NGC 1960. In this connection, its least kinematic probability (as per GAIA database) also confirms it as a field Star. Although, its position in $(U-B)\ vs\ (V-B)$ TCD is found just on the main sequence as depicted in Fig. 16.

Author has selected two stars, ID 2352 ($5^h : 36^m : 03.82^s, +34^0 : 11^{'} : 51.5^{''}$) and ID 2379 ($5^h : 36^m : 12.86^s, +34^0 : 07^{'} : 54.1^{''}$), to compare their light curves with those of variable star V_{16}. Both stars show approximate constant magnitude difference

during entire observation sessions. Although, their light curves have character of Long Periodic Variables, but seems to be instrumental effect. As per observations of each individual night, their magnitude variation less than that of the variable star V_{16} as shown in upper panels of Fig. 9. The pixel distances of these stars (IDs 2323, 2352, 2379) indicate that they are far from each other, as listed in Table 6. Colour, $(B-V)_o$, values of V_{16} and ID 2352 are close to each other, but away from that of ID 2379. Thus, the similar character of light curves for ID 2352 and ID 2379 confirms colour- free selection of comparison stars during time series analysis via absolute photometry.

9.7.5 Star IDs 2439, 2451 (V_{17}) and 2479 of NGC 1960

The values of distance and kinematic probability for the variable star V_{17} are found to be $1.107\pm0.055\ kpc$ and 0.771 respectively. Consequently, it is assigned as a member of cluster and found near the main sequence as shown in Fig. 16. Author did not find any sign of regular pulsation for it. A speck of stellar brightness for this variable star has detected on date 11 December 2013 as depicted in Fig. 9. The period of this variable star can not be computed by the codes of 'PERIOD04' and 'PerSea'. Thus, this variable star is suggested to be an irregular type variable.

In the case of variable star V_{17}, the comparison stars are ID 2439 ($5^h:36^m:14.60^s,\ 34^o:07^{'}:21.1^{''}$) and ID 2479 ($5^h:35^m:56.35^s,\ 34^o:05^{'}:53.3^{''}$). The comparative light curves of both comparison stars show almost constant difference of brightness during observation of each night. Comparative light curves of V_{17} with its comparison stars indicate that spacing between their light curves varies night to night as depicted in the middle Set of Panels of Fig. 9. It may be due to character of long variability of V_{17} with irregular pulsation. In addition, the light curves of star ID 2439 also show a character of long term variability.

9.7.6 Star IDs 2868, 2875 (V_{18}) and 2889 of NGC 1960

The variable star V_{18} is a cluster member due to its kinematic probability (0.764) of membership and distance $(1.191\pm0.065\ kpc)$. The light curves of variable star V_{18} show no sign of periodic pulsation. As per observation on date 11 December 2013, flare type structure has been detected in the constructed light curve of this variable star. Its location is found near the main sequence in $(U-B)$ vs $(B-V)$ TCD and depicted in Fig. 15. The codes of 'PERIOD04' and 'PerSea' are not able to compute period for this variable star. Consequently, it is classified as an irregular variable star with eruptive phenomena.

In the case of V_{18}, the comparison stars are ID 2868 ($5^h:36^m:34.54^s,\ 34^o:08^{'}:31.6^{''}$) and ID 2889 ($5^h:35^m:55.53^s,\ 34^o:07^{'}:52.2^{''}$). Due to the almost constant brightness in the light curves for star ID 2868, it is assigned as a stable star. The black comparative light curves of field stars shows no noticeable fluctuation in flux, whereas, comparative light curves of V_{18} variable and field stars confirm the long term stellar variability of V_{18} as depicted in the lower set of panels of Fig. 9.

9.8 Characteristics test of $\delta-Scuti-\gamma-Doradus$ hybrid variables

Generally, $\gamma-Doradus$ instability strip is found below the $\delta-Scuti$ strip. Several authors pointed out that some portion of instability strips of both these classes overlap each other. Such hybrid candidates have already been discovered in open clusters [32, 43]. The estimated log(age) of cluster NGC 1960 is $7.35\pm0.05\ yr$ and found close to J20. It belongs to a young open cluster in which the A/F-type stars have not evolved. $\delta-Sct$ stars have high pulsation mode frequencies ($\nu\geq35\ d^{-1}$) as inferred from theoretical models [44]. Such fast variability should be detectable in the light curves, except for the fact that the amplitudes are very small.

9.8.1 Star IDs 592, 595 and 600 (V_1) of NGC 1960

Author has selected two stars, ID 592 ($5^h:36^m:39.44^s,\ +34^0:06^{'}:12.3^{''}$) and ID 595 ($5^h:36^m:41.27^s,\ +34^0:09^{'}:29.9^{''}$), to compare their light curves with the Star ID 600 and these stars are marked by C1(V1) and C2(V1) in Fig.13. Joshi et al. 2020 [32] assigned ID 595 as a cluster member and a hybrid $\delta\ Scuti\ \gamma\ Daradus$ variable star and denoted it by V_{27} in their analysis. It has the lowest V-magnitude and colour (B-V) of all stars, listed in Table 5. Upon inspection of light curves of Star IDs 592 and 595 in Fig. 4, the author noted that both stars showed a approximate

similar pattern. The light curves of ID 595 have a regular pattern of flux variation with very low amplitude and the author considered it as an effect of instrumental pseudo-variability. Thus, it is impossible to find character of young $\delta - Scuti$ stars based on low quality data sets. The light curves of star ID 600 have shown prominent variation in its magnitude. Its period is found to be $0.3057\pm0.0815\ d$ and $0.4000\pm0.1055\ d$ by the codes of 'PERIOD04' and 'PerSea', respectively. These value are similar to data strings. As a result, author did not advocated about its true period. It has characteristics similar to the variable star V_4 star and it is listed as miscellaneous in the present analysis. Its location within cluster is shown by the mark M36(V1) in Fig. 2. It is also found to be more kinematic probabilistic member of the cluster.

9.8.2 Star IDs 678, 688 (V_4) and 694 of NGC 1960)

Star IDs 678 ($5^h:36^m:33.38^s,\ +34^0:10^{'}:13.0^{''}$) and 694 ($5^h:36^m:37.21^s,\ +34^0:12^{'}:39.3^{''}$) are selected as possible comparison stars. These stars are marked by C1(V4) and C2(V4) in Fig. 13 and their physical coordinates are found closest compare than other set of stars. Variable star V_4 is assigned to be a $\gamma\ Daradus$ variable star with period $1.07066\ d$ and marked by V_{62} in the work of JO20. In the present analysis, its period is found to be $0.3115\pm0.1168\ d$ by the code of 'PERIOD04', whereas the said value is $0.2857\pm0.0706\ d$ by the ANOVA analysis as per code of 'PerSea'. These values are closed to average length of data strings. It is more kinematic probabilistic member of cluster and marked by M36(V4) in Fig. 2. In present study, author did not classify it due to circumstances of data.

The trend of light curves of Star IDs 678 and 694 are approximately similar to each other. However, light curves of star ID 694 show a regular feature of short periodic variability and it is considered to be pseudo-variability by author.

10 RESULTS AND DISCUSSION

The contamination of fluxes of fainter stars is occurred due to their nearby brighter stars. Author also found very high scattering of data points in the light curves of brighter stars of NGC 1960 due to saturation limit of pixels of CCD camera in the present deep photometric observations. As a result, author did not analysis the time series observations of bright and their nearby stars.

Star IDs 1124, 1197, 1348 and 2868 of M36 have approximately constant stellar magnitude during whole observations, their celestial coordinates are ($5^h:36^m:28.92^s,\ 34^o:13^{'}:23.2^{''}$), ($5^h:36^m:25.21^s,\ 34^o:13^{'}:04.1^{''}$), ($5^h:36^m:29.70^s,\ 34^o:04^{'}:53.6^{''}$) and ($5^h:36^m:34.54^s,\ 34^o:08^{'}:31.6^{''}$) respectively. Thus, these stars are classified as the stable stars within cluster. According to the GAIA database, the distances of stars 1124, 1197, 1348 and 2868 have been computed as $1.166\pm0.035\ kpc$, $1.152\pm0.036\ kpc$, $3.461\pm0.278\ kpc$ and $1.419\pm0.109\ kpc$ respectively. Thus, star IDs 1124 and 1197 are members of cluster NGC 1960.

In the present analysis, some variable stars (such as V_2) show two distinct period values via two distinct algorithm (ANOVA and statistical analysis. In the case of variable star V_2, period value via statistical analysis is close to the length of individual data strings in 2015, therefore it is not suitable to consider a true period. As a result, true period for variable star V_2 is $0.6250\pm0.0274\ d$ as per ANOVA analysis.

One $\gamma - Dor$, one RR Lyre, two EB, two Ellipsoidal, two hybrid ($\delta\ Scuti - \gamma - Dor$), two LADS, two rotational and six irregular or miscellaneous type variable stars are reported in the present work.

Among the 18 detected variable stars, only four are cross matched with JO20, whereas three of the 36 selected comparison stars are cross matched with variable stars of JO20, whom stellar variability is not confirmed in the present analysis. Thus, we concluded that the time series data of one night could lead to an over-estimation of short periodic variables via absolute/standard phtotmetry.

JO20 used continuous time series data less than 3.5 hours for each observational night, whereas author has additional time series data of 5.4, 7.6, 7.2 and 5.6 hours as observed on dated 11-12-2013, 20-12-2013, 12-01-2015 and 08-02-2015 respectively. Since period value of variable star V_2 of M36 by JO20 appears to be inaccurate in the view of additional data, therefore it is best to avoid to classifying variable stars, that have

approximately same/ slightly longer period than the time duration of observation for a particular night.

The light curves for selected comparison stars of M36 have been constructed by absolute photometry via SSM approach. Their comparative analysis indicates that absolute photometry is a meaningful to search for variable stars in the target filed. SSM approach gave similar trends of pseudo-variability for comparison stars in the field of studied cluster. As a result, this approach confirms that resulting light curves of comparison stars do not depend on the nature of reference catalogue produced by standard magnitudes of stars.

Author concludes that the detection process of short-period variability shorter than a single night has nothing to do with the absolute/standard photometry. Although, the appearance of a unique feature in light curves of potential variable star is confirmed through the differential photometry of similar stars.

11 CONCLUSION

The present analysis is devoted the detection of short periodic variable stars with periods less than 1 day. In this connection, author did not present any analysis for the classification of potential candidate of variable stars characterized by long periodicity and irregular variability. To find small periodic variables, time series data for NGC 1960 have been collected over five nights of observations. In this connection, the stellar light curves for NGC 1960 have been extracted from these time series data.

By deep investigate of stellar light curves, a total of 18 variable stars have been identified in the field of view of cluster NGC 1960.

Four of these 18 variable stars are cross matched with JO20. In addition, other three variable stars of JO20 are not found to be short pulsation stars in present analysis. To perform membership analysis for variable stars, the mean proper motion of NGC 1960 in their RA and DEC directions were estimated as ($0.314\pm0.026\ mass/yr$ and $-2.333\pm0.037\ mass/yr$), respectively.

The gap of time duration (1.2 yr) seems too enough to accurately determine the Period of any variable star. As per 10 cases out of 18 for NGC 1960 (V_1, V_3, V_4, V_5, V_8, V_9, V_{13}, V_{14}, V_{15} and V_{16}), most derived periods are 0.25-0.30 days in length, this is the average length of the individual data strings in 2013 and 2015. This makes the period determination very suspicious. Thus, the large gap in between the nights (almost 1 yr) causes additional aliases. As a result, author concludes that it is impossible to determine the true periods, and the physical reason of the light variability based on such scare data sets poorly dispersed over a long period of time.

Due to the observational limitations of CCD camera of 1.04 m telescope at ARIES, a telescope equipped with a very high-capacity CCD camera is needed to carry out the task of searching for a signal of variability in the brighter stars of NGC 1960.

DISCLAIMER

This paper is an extended version of a preprint document of the same author. The preprint document is available in this link: https://assets.researchsquare.com/files/rs-1895965/v3_covered_2ee227f7-6bc1-41c0-901c-57bc97b83064.pdf?c=1688404350 [As per journal policy, preprint article can be published as a journal article, provided it is not published in any other journal].

ACKNOWLEDGEMENT

GCJ acknowledges the web-portal services of SIMBAD, VIZIER and ESO. Collection and observation of time series data for studied cluster NGC 1960 is performed by GCJ during 18 September 2012 to 27 April 2015. Director, ARIES gave permission to GCJ to use ARIES Data for research work via letter no. AO/2018/41 on date 12 April 2018.

COMPETING INTERESTS

Author has declared that no competing interests exist.

REFERENCES

[1] Luo YP, Zhang XB, Deng LC, Han ZW. Discovery of 14 new slowly pulsating b stars in the open cluster NGC 7654, ApJ Letters. 2012;746:L7.

[2] Dupret MA, Grigahcene A, Garrido R, Gabriel M, Scuflaire R. Theoretical instability strips for δ Scuti and γ Doradus syars, A&A. 2004;414(2):L17.

[3] Sharma S, Pandey AK, Ogura K, Mito H, Tarusawa K, Sagar R. Wide-field CCD photometry around nine open clusters. The Astronomical Journal. 2006;132(4):1669.

[4] Cantat-Gaudin T, Anders F. Clusters and mirages: Cataloguing stellar aggregates in the Milky Way. Astronomy Astrophysics. 2020;633:A99.

[5] Joshi, Gireesh C, Tyagi RK. Statistical analysis for precise estimation of Structural Properties of NGC 1960, Mathematical Sciences Int Research Journal. 2015;4:384.

[6] Barkhatova KA, Zokharova PE, Shaskina LP, Oreknova LK. Some Kinematic parameters of open cluster systems, Astron. Zh., 1985;62:854.

[7] Conrad C, Scholz RD, Kharchenko NV, Piskunov AE, Röser S, Schilbach E, De Jong RS, Schnurr O, Steinmetz M, Grebel EK, Zwitter T. A RAVE investigation on Galactic open clusters-II. Open cluster pairs, groups and complexes. Astronomy & Astrophysics. 2017;600:A106.

[8] Hasan P, Kilambi GC, Hasan SN. Near Infrared Photometry of the Young star clusters NGC 1960, NGC 2453 and NGC 2384, Bull. Astr. Soc. India. 2005;33:151.

[9] Jeffries RD, Naylor T, Mayne NJ, Bell CPM, Littlefair SP. A lithium depletion boundary age of 22 Myr for NGC 1960, MNRAS. 2013;434(3):2438.

[10] Johnson HL, Morgan WW. Fundamental stellar photometry for standards of spectral type on the Revised System of the Yerkes Spectral Atlas, Astrophysical Journal. 1953;117:313.

[11] Kharchenko NV, Piskunov AE, Roeser S, Schilbach E, Schola RD. Astrophysical supplements to the ASCC-2.5 II. Membership probabilities in 520 Galactic open cluster sky areas, Astron. Nachr., 2004;325:740.

[12] Nilakshi, Sagar R, Pandey AK, Mohan V. A study of spacial structure of galactic open star clusters, A&A. 2002;383:153.

[13] Sanner J, Altmann M, Brunzendorf J, Geffert M. Photometric and kinematic studies of open star clusters. II. NGC 1960 (M 36) and NGC 2194, A&A. 2000;357:471.

[14] Sharma S, Pandey AK, Ogura K, Aoki T, Pandey K, Sandhu TS, Sager R. Mass functions and photometric binaries in nine open clusters, AJ. 2008;135:1934.

[15] Delgado AJ, Alfaro EJ, Garrido R, Garcia-Pelayo JM. Search for B-Type variables stars in open clusters, Information Bullatine on Variable Stars(IBVS). 1984;2603:1.

[16] Smith R, Jeffries RD. Dust discs around intermediate-mass and Sun-like stars in the 16 Myr old NGC 1960 open cluster. Monthly Notices of the Royal Astronomical Society. 2012;420(4):2884-98.

[17] Joshi YC, Joshi S, Kumar B, Mondal S, Balona LA. MNRAS. 2012;419:2379.

[18] Landolt AU. AJ. 1992;104:340.

[19] Stetson PB. DAOPHOT: A computer program for crowded-field stellar photometry. Publications of the Astronomical Society of the Pacific. 1987 Mar 1;99(613):191.

[20] Stetson PB. In ASP conf. Ser. vol. 25, Astronomical Data Analysis Software and System, I. Astron. Soc. Pac., ed. Warrall D. M., and Biemesderfer C., Barnes J., San Francisco. 1992;297.

[21] Joshi, Gireesh C. Dynamic Properties and Search of Variable Stars: NGC 1960, In: Mishra, G.C. editor. National Conference on Innovative Research in Chemical, Physical, Mathematical Sciences, Applied Statistics and Environment Dynamics (CPMSED-2015), Krishi Sanskriti Publications (New Delhi) ISBN: 978-93-85822-07-0. 2015;22-27.

[22] Sariya DP, Lata S, Yadav RK. Variable stars in the globular cluster NGC 4590 (M68). New Astronomy. 2014 Feb 1;27:56-62.

[23] Wood PR, Sebo KM. On the pulsation mode of Mira variables: evidence from the Large Magellanic Cloud. Monthly Notices of the Royal Astronomical Society. 1996;282(3):958-64.

[24] Lata S, Yadav RK, Pandey AK, Richichi A, Eswaraiah C, Kumar B, Kappelmann N, Sharma S. Main-sequence variable stars in Young open cluster NGC 1893, MNRAS. 2014;442(1):273.

[25] Lomb N. Least-squares frequency analysis of unequally spaced data, AP&SS0. 1976;39(2):447

[26] Scargle JD. Studies in astronomical time series analysis. II-Statistical aspects of spectral analysis of unevenly spaced data. Astrophysical Journal, Part 1, vol. 263, Dec. 15, 1982, p. 835-853. 1982;263:835-53.

[27] Kovács G, Zucker S, Mazeh T. A box-fitting algorithm in the search for periodic transits. Astronomy Astrophysics. 2002;391(1):369-77.

[28] Plavchan P, Jura M, Kirkpatrick JD, Cutri RM, Gallagher SC. Near-infrared variability in the 2MASS calibration fields: A search for planetary transit candidates. The Astrophysical Journal Supplement Series. 2008;175(1):191.

[29] Ransom SM, Eikenberry SS, Middleditch J. Fourier techniques for very long astrophysical time-series analysis. The Astronomical Journal. 2002 Sep 1;124(3):1788.

[30] Meurers J. Ein Stern-Aggregat im M 36. Mit 7 Textabbildungen. Zeitschrift für Astrophysik. 1958;44:203.

[31] Chian BT, Zhu GL. An Investigation on the Proper-Motions of the Open Clusters NGC1960 NGC6530 and NGC7380. Shanghai Observatory Annals. 1966;26:63.

[32] Joshi YC, Maurya J, John AA, Panchal A, Joshi S, Kumar B. Photometric, kinematic, and variability study in the young open cluster NGC 1960. Monthly Notices of the Royal Astronomical Society. 2020;492(3):3602-21.

[33] Gaia collaboration et al., A&A. 2016;595:A2.

[34] Gaia collaboration et al., A&A. 2021;649:A1

[35] Joshi GC. Implication of Phase-folded Diagrams for Validation of the Nature of Stellar Variability I: the case of NGC 6866. Bulgarian Astronomical Journal. 2022;37(01).

[36] Hanson MM, ZAMS O Stars, (Boulder-Munich II: Properties of Hot, Luminous Stars, Edited by Ian) ASP Conference Series. 1998;131-1.

[37] Balona LA, Guzik JA, Uytterhoeven K, Smith JC, Tenenbaum P, Twicken JD. The Kepler view of Doradus stars. Monthly Notices of the Royal Astronomical Society. 2011;415(4):3531-8.

[38] Clement CM, Muzzin A, Dufton Q, Ponnampalam T, Wang J, Burford J, Richardson A, Rosebery T, Rowe J, Hogg HS. Variable stars in Galactic globular clusters. The Astronomical Journal. 2001;122(5):2587.

[39] Luo YP. Variable stars in the open cluster NGC 2141, RAA. 2015;15(5):733.

[40] Catelan M, Pritzl BJ, Smith HA. The rr lyrae period-luminosity relation. i. theoretical calibration. The Astrophysical Journal Supplement Series. 2004;154(2):633.

[41] Balona LA, Baran AS, Daszyńska-Daszkiewicz J, De Cat P. Analysis of Kepler B stars: rotational modulation and Maia variables. Monthly Notices of the Royal Astronomical Society. 2015;451(2):1445-59.

[42] Samus' NN, Kazarovets EV, Durlevich OV, Kireeva NN, Pastukhova EN. General catalogue of variable stars: Version GCVS 5.1. Astronomy Reports. 2017;61:80-8.

[43] Hartman JD, Gaudi BS, Holman MJ, McLeod BA, Stanek KZ, Barranco JA, Pinsonneault MH, Kalirai JS, Deep MMT Transit Survey of the Open Cluster M37. II. Variable Stars., The Astrophysical Journal. 2008;675:1254.

[44] Michel E, Dupret MA, Reese D, et al., What CoroT tells us about $\delta - Scuti$ stars-Existence of a regular pattern and seismic indicates to characterize stars, EPJ Web Conferences. 2017;160:03001.

Peer-review history:
The peer review history for this paper can be accessed here:
https://www.sdiarticle5.com/review-history/104555